AFRL-ML-WP-TR-2002-4049

INTELLIGENT CONTROL SYSTEMS FOR HOT FORGING AND EXTRUSION PROCESSES

Dr. Anil B. Chaudhary

UES, Inc.
4401 Dayton-Xenia Road
Dayton, OH 45432-1894

NOVEMBER 1994

Final Report for 01 June 1994 – 31 October 1994

THIS IS A SMALL BUSINESS INNOVATION RESEARCH (SBIR) PHASE 1 REPORT

Approved for public release; distribution is unlimited.

20030304 037

MATERIALS AND MANUFACTURING DIRECTORATE
AIR FORCE RESEARCH LABORATORY
AIR FORCE MATERIEL COMMAND
WRIGHT-PATTERSON AIR FORCE BASE, OH 45433-7750

NOTICE

Using government drawings, specifications, or other data included in this document for any purpose other than government procurement does not in any way obligate the U.S. Government. The fact that the government formulated or supplied the drawings, specifications, or other data does not license the holder or any other person or corporation; or convey and rights or permission to manufacture, use, or sell any patented invention that may relate to them.

This report has been reviewed by the Office of Public Affairs (ASC/PA) and is releasable to the National Technical Information Service (NTIS). At NTIS, it will be available to the general public, including foreign nations.

This technical report has been reviewed and is approved for publication.

JAMES C. MALAS
Project Engineer
Process & Fabrication Branch

Copies of this report should not be returned unless return is required by security considerations, contractual obligations, or notice on a specific document.

REPORT DOCUMENTATION PAGE

The public reporting burden for this collection of information is estimated to average 1 hour per response, including the time for reviewing instructions, searching existing data sources, searching existing data sources, gathering and maintaining the data needed, and completing and reviewing the collection of information. Send comments regarding this burden estimate or any other aspect of this collection of information, including suggestions for reducing this burden, to Department of Defense, Washington Headquarters Services, Directorate for Information Operations and Reports (0704-0188), 1215 Jefferson Davis Highway, Suite 1204, Arlington, VA 22202-4302. Respondents should be aware that notwithstanding any other provision of law, no person shall be subject to any penalty for failing to comply with a collection of information if it does not display a currently valid OMB control number. **PLEASE DO NOT RETURN YOUR FORM TO THE ABOVE ADDRESS.**

1. REPORT DATE *(DD-MM-YY)*	2. REPORT TYPE	3. DATES COVERED *(From - To)*
November 1994	Final	06/01/1994 – 10/31/1994

4. TITLE AND SUBTITLE	5a. CONTRACT NUMBER
INTELLIGENT CONTROL SYSTEMS FOR HOT FORGING AND EXTRUSION PROCESSES	F33615-94-C-5807
	5b. GRANT NUMBER
	5c. PROGRAM ELEMENT NUMBER 65502F

6. AUTHOR(S)	5d. PROJECT NUMBER
Dr. Anil B. Chaudhary	3005
	5e. TASK NUMBER 05
	5f. WORK UNIT NUMBER 9S

7. PERFORMING ORGANIZATION NAME(S) AND ADDRESS(ES)	8. PERFORMING ORGANIZATION REPORT NUMBER
UES, Inc. 4401 Dayton-Xenia Road Dayton, OH 45432-1894	UES-TR-95-ABC

9. SPONSORING/MONITORING AGENCY NAME(S) AND ADDRESS(ES)	10. SPONSORING/MONITORING AGENCY ACRONYM(S)
Materials and Manufacturing Directorate Air Force Research Laboratory Air Force Materiel Command Wright-Patterson Air Force Base, OH 45433-7750	AFRL/MLLP
	11. SPONSORING/MONITORING AGENCY REPORT NUMBER(S) AFRL-ML-WP-TR-2002-4049

12. DISTRIBUTION/AVAILABILITY STATEMENT
Approved for public release; distribution is unlimited.

13. SUPPLEMENTARY NOTES
THIS IS A SMALL BUSINESS INNOVATION RESEARCH (SBIR) PHASE 1 REPORT

14. ABSTRACT *(Maximum 200 Words)*

The Phase I effort on Intelligent Metal forming Processes was performed with the objective of determining feasibility of the application of process control technology within the forming industry. The result of this development was a three-stage approach to velocity control for microstructual optimization. The overall work effort was divided into three components: (1) Development of open-loop control procedure for forming processes, (2) Industrial consortium development and market technical survey on the most important process control needs, and (3) Development of specifications for the neutral data to facilitate open-loop control with a multitude of control objectives. The Phase II effort plan will be developed in response to the recommendations of the industrial consortium so as to make maximum impact on the U.S. manufacturing industry.

15. SUBJECT TERMS

Thermomechanical Processing, Open-Loop Control, Process Control, Optimal Design, Microstructure Control, Forge Equipment Modeling, SBIR Report

16. SECURITY CLASSIFICATION OF:			17. LIMITATION OF ABSTRACT:	18. NUMBER OF PAGES	19a. NAME OF RESPONSIBLE PERSON (Monitor)
a. REPORT Unclassified	b. ABSTRACT Unclassified	c. THIS PAGE Unclassified	SAR	54	Dr. James C. Malas 19b. TELEPHONE NUMBER *(Include Area Code)* (937) 255-9803

TABLE OF CONTENTS

1.0   INTRODUCTION

In designing metalworking processes, the most important task is the selection of the controlling process parameters which will ensure the required part quality along with specific mechanical and physical characteristics. Controlling process parameters are the number and sequence of material flow operations, the heat treating conditions, and the associated quality assurance tests. When designing unit manufacturing processes, special features such as nonlinear, irreversible finite-deformation flow must be considered. Simultaneously, the complex interdependence of the process parameters and their effect on the finished part quality, reliability and inspectibility must be considered. Considering the involved overall complexity, this project - **the development of an Intelligent Control and Optimal Design System for Metal Forming Processes** - is the right thrust at the right time. This is because forming process simulation tools, previously considered a luxury, are now becoming accepted as a necessity by the industry. By using simulation technology, companies can shift the trial and error design of the forming process from the shop floor to the computer (see Figure 1). This computer trial and error is highly useful in reducing the overall design cost and providing substantially improved insight in the forming process. Now, however, the time has come to minimize this trial and error in the computer so that the design engineer may focus the effort in finding optimal solutions rather than finding one that just simply works. This is seen as a major advance which will render the 'old' simulation procedure obsolete.

The most significant roadblock for implementation of these simulation technologies has been the requirement of excessive human intervention for process model generation. However, with the advent of the 2D and 3D automatic remeshing algorithms which are currently available commercially to the forming industry, the pathway to determination of optimal design solution is seen to be clear. It is now feasible to draw upon the principles of control theory and optimization and merge them effectively with computational mechanics to arrive at a powerful numerical solution strategy for design of a wide variety of forming processes.

UES has performed the SBIR Phase I effort under Contract F33615-94-C-5807 with the objective of determining feasibility of the application of process control technology within the forming industry. The result of this effort was the development of a three-stage approach to ram velocity control for microstructural optimization during the forming process as described in Figure 2. The work in Phase I was divided into the following tasks:

1.   Open Loop Control of TiAl IBR forging: This component geometry was originally forged with a nickel base superalloy at Pratt and Whitney. The tooling for this process is available to the Wright Laboratory. The computer model TiAl material forging of the same geometry showed difficulties with respect to overloading of the tools. Another difficulty was observed due to the lack of recrystallization in the hub region (see Figure 3). As a result, the forming process was reorganized into two stages. The first operation is to be for billet conditioning in which the required microstructure will be evolved during forming. The second stage is to be for the
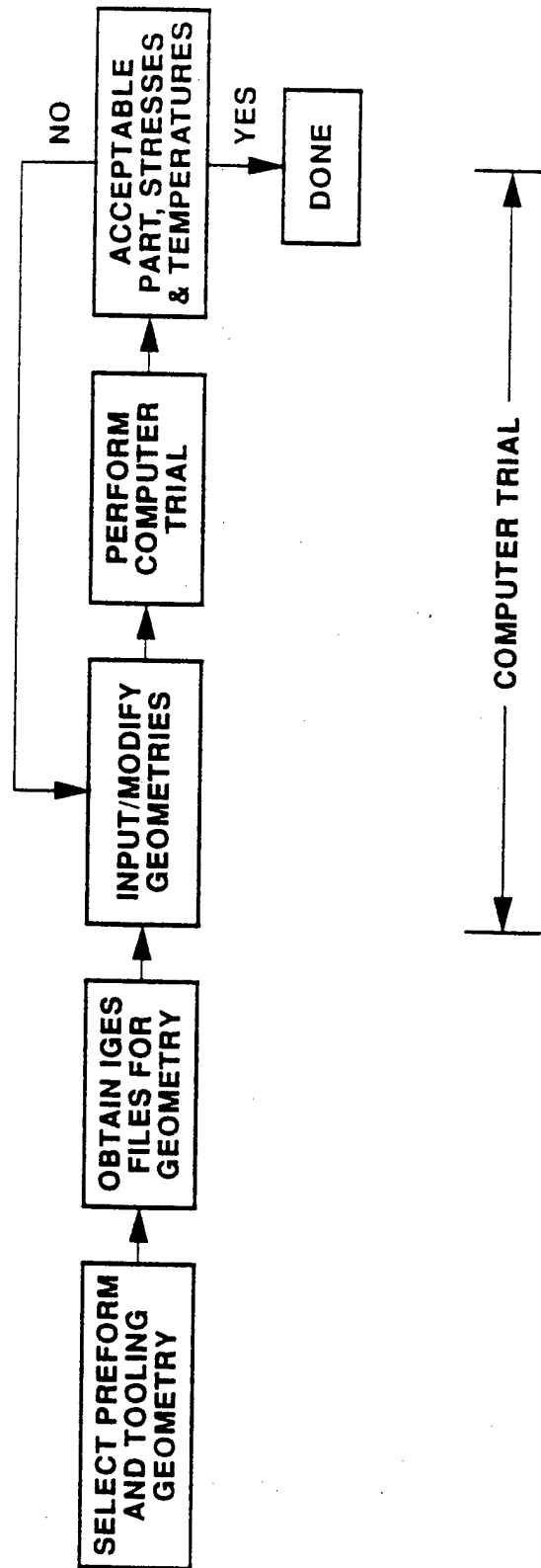
1

Figure 1. Trial and Error on the Computer to Obtain Acceptable Design.

THREE STAGE APPROACH

Desired Product Microstructure

Microstructure Model and Optimization Procedure

Strain Rate Trajectory

Process Model (FEM Simulation) and Optimization

Ram Velocity Trajectory

Equipment or Equipment Model or Equipment Simulation

Actual or Simulated Product Microstructure
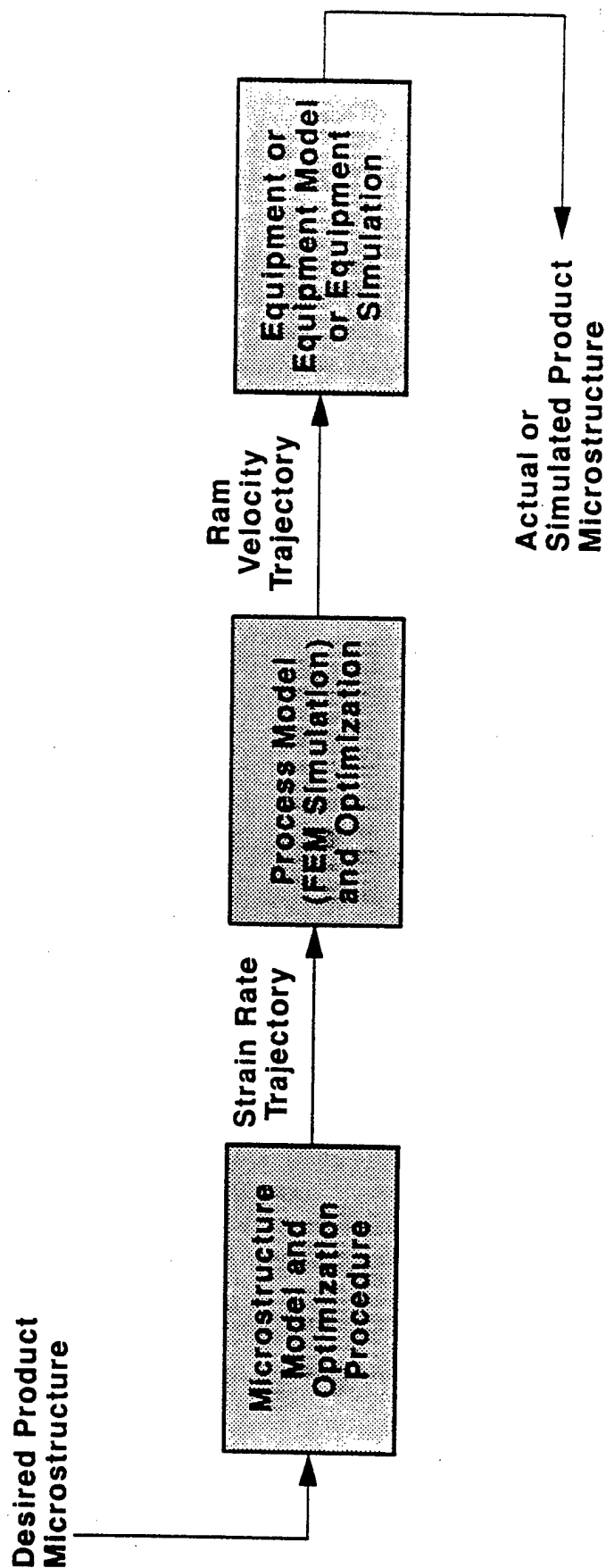
Figure 2. Three Stage Approach to Forming Process Control.

3

100.0000	
94.0000	
88.0000	
92.0000	
76.0000	
70.0000	
64.0000	
58.0000	
52.0000	
46.0000	
40.0000	
34.0000	
28.0000	
22.0000	
16.0000	
10.0000	

PERCENT RECRYSTALLIZED CONTOUR
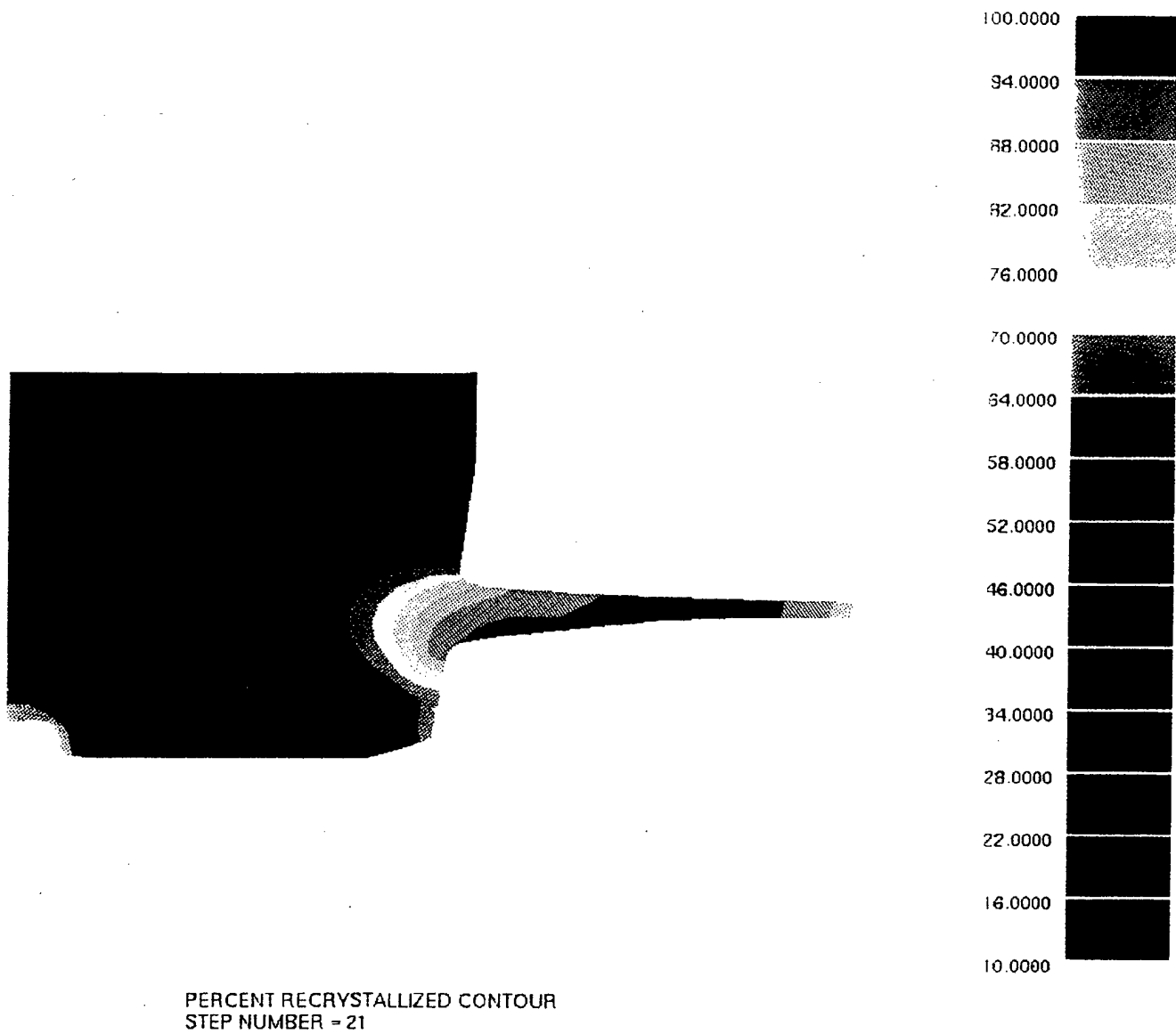STEP NUMBER = 21

Figure 3. Lack of Recrystallization in the Hub Region for a Direct Single Step
Forging Operation.

shaping operation. The billet conditioning process was designed using the cost function based optimization algorithm. The resultant distribution of the grain size and percent recrystallization for the gamma TiAl material after billet conditioning is shown in Figure 4.

2.   Development of Neutral Data Interface Specification: The Phase I effort determined that the neutral data interface specification as an independent module becomes necessary to support the process solver due to its size and complexity. The necessary contents of this interface were determined based upon the market technical survey. The modules for optimal material deformation trajectory determination and the equipment control are to have independent access to the neutral data specification in order to perform their respective interaction tasks.

3.   Consortium Development and Market Technical Survey: An important objective of Phase I effort was to evaluate the impact of the existing technology for process control on the industry and then determine the direction for further development such that maximum benefit may be derived. This was accomplished through a technical workshop at Wright Laboratory which was attended by representatives from a wide range of industries covering the entire spectrum of the forming industry (see Figure 5). The Phase I technical effort was discussed at length with the participants. This process control research was received with much enthusiasm and several recommendations were obtained for effectively performing further research in this area such that it would directly improve their competitiveness. In addition, the Market Technical Survey was performed through individual inquires. The responses of this technical survey is a major driver for the Phase II effort.

In the following document, Section 2 contains the technical approach utilized for the open loop control procedure. Section 3 contains the specifications for the neutral data interface. Section 4 contains the recommendations obtained from the Market Technical Survey. Section 5 summarizes the accomplishments of this Phase I effort. Appendix A contains a technical document on the utilization of the open-loop control procedure for control of microstructure and Appendix B contains the technical procedure for optimal material deformation trajectory determination.
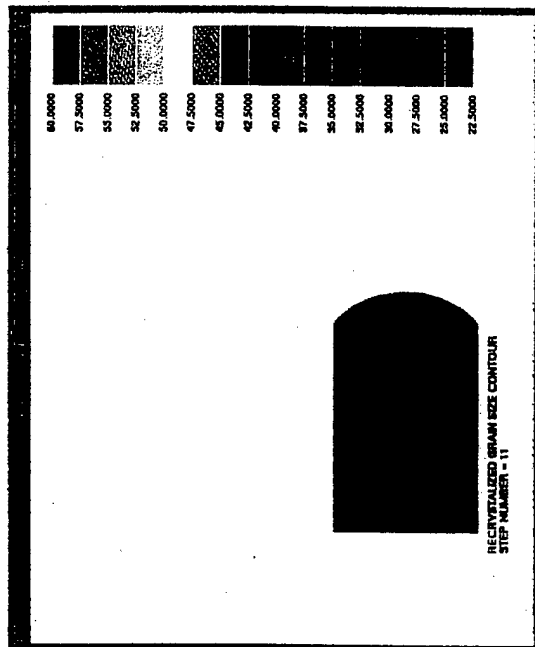
(a)
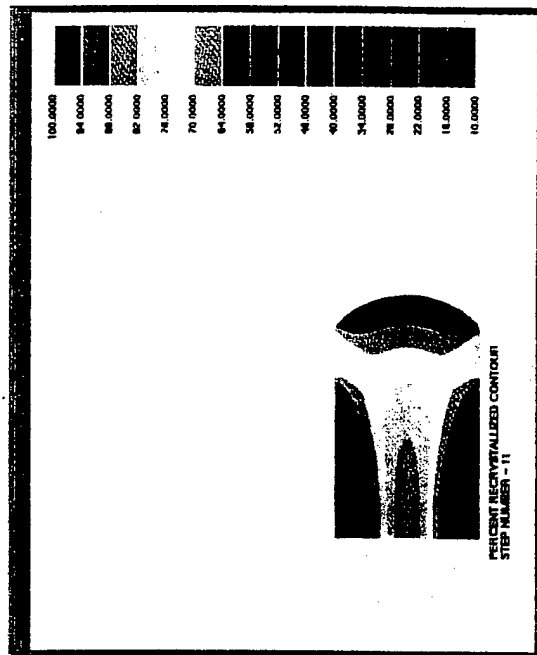
(b)

Figure 4. Results of Controlled Upsetting of Billet to Create Preform for an IBR Component.

ORGANIZATION	TYPE OF BUSINESS
AC DELCO	Automotive
BethForge, Inc.	Primary Process
Braun Enginerring	Automotive
Colfor	Automotive
Danaher Tool Group	Hand Tools
Emhart Corporation	Fasteners
Ford Motor Company	Automotive
General Electric/Power Generation Division	Aerospace
General Motors Saginaw Division	Automotive
Henry Vogt Machine Company	Automotive
Kaiser Aluminum	Aerospace/Automotive
Ladish	Aerospace
MASCO Corporation	Automotive
MECONS	Consultant
Pratt & Whitney	Aerospace
Rockwell International	Automotive
Snap-On Tools	Hand Tools
Teledyne Allvac	Aerospace/primary processing

Figure 5.   Technical Workshop Attendees.

2.0   OPEN-LOOP CONTROL OF MATERIAL DEFORMATION TRAJECTORY

The basic objective of this effort is to determine a variable ram velocity such that material will follow desired deformation path and thereby result in the desired grain size and maximum percent recrystallization upon completion of the forming operation. This is applicable within the aerospace industry for isothermal forming operations using a hydraulic press.

A three stage approach was developed to this end as shown in Figure 2. The first stage involved calculation of optimal material deformation trajectory with a specific microstructural goal. The second stage involved utilizing an optimization loop in conjunction with the process model to ensure that the requisite strain-rate variation is enforced within the material deforming region. The basic logic underlying the optimization procedure is shown in Figure 6.. This technology was utilized for determination of optimal forging parameters for billet conditioning for an IBR component (see Figure 4). This procedure was also utilized to control the material strain rate within the desired window for a disk forging problem (see Figure 7).

The developed methodology under the Phase I of the SBIR project is currently available as an integrated implementation. This would be enhanced in the Phase II effort to include limits on the rate of change of ram velocity depending on equipment capabilities. This would be the first candidate for technology transfer within an aerospace related business.

3.0   DEVELOPMENT OF NEUTRAL DATA INTERFACE

The primary objective behind the neutral data interface is to permit the individual development in controls, microstructural modeling and process simulation progress independently (see Figure 8). The basic difficulty arises from the interdisciplinary nature of the process control research. Given that this technical effort brings together the fields of materials science, control algorithms and process model, the common information needed by the different phases of computations needs to be accessible in a suitable manner. Referring to Figure 2, the neutral data interface is essentially the software which will permit error-free data interchange between the different stages of the control/optimization sequence.

Since the process model needs to account for a large number of physical phenomena which take place during the forming process, the software for its modeling is quite complex. The ANTARES software, which will be utilized for the process simulation task, contains the process solver as well as meshing and remeshing components which execute in tandem. The simulation information is transferred from one mesh to the next as the material deformation progresses to higher levels of severity. This makes for a large complexity for extracting information out of the process solver results database. As a result, the neutral data interface will be built on top of the process solver.
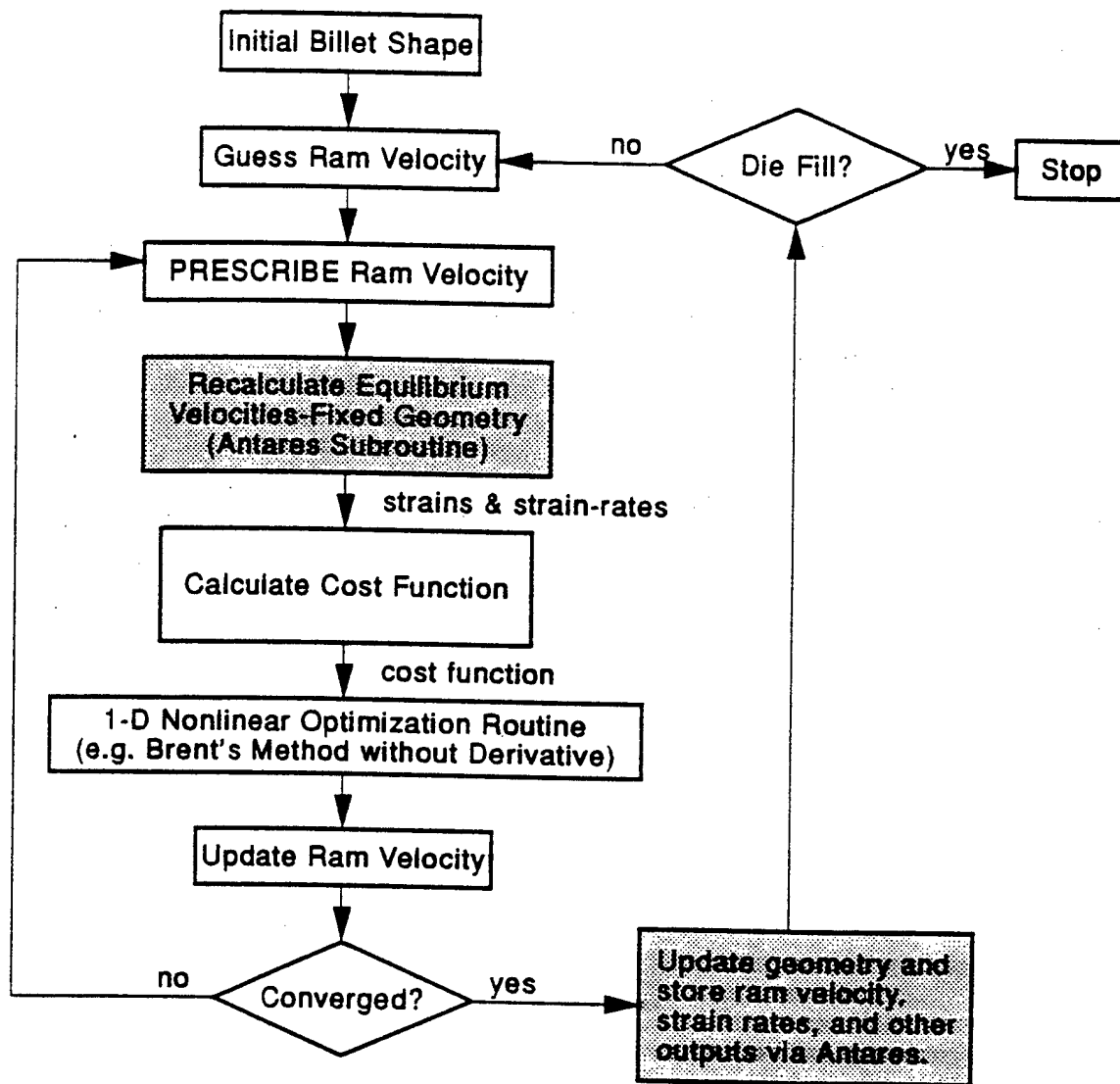
8

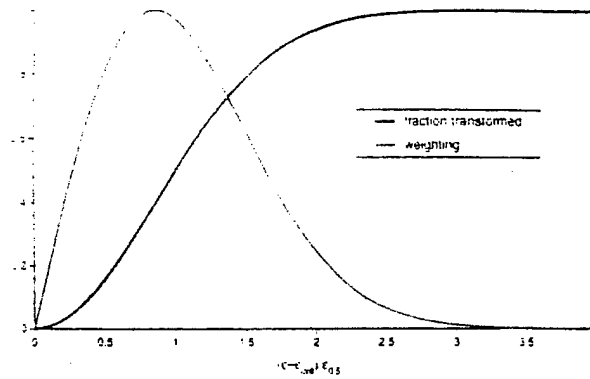Figure 6. Optimization Using the Univariate Search Method.

9

Cost Function

Microstructure and Weighting

- Desire Uniform, Constant, Strain Rate During Transformation:

$$J = \sum_{billet} W(\varepsilon)(\dot{\varepsilon} - \dot{\varepsilon}_{des})^2$$
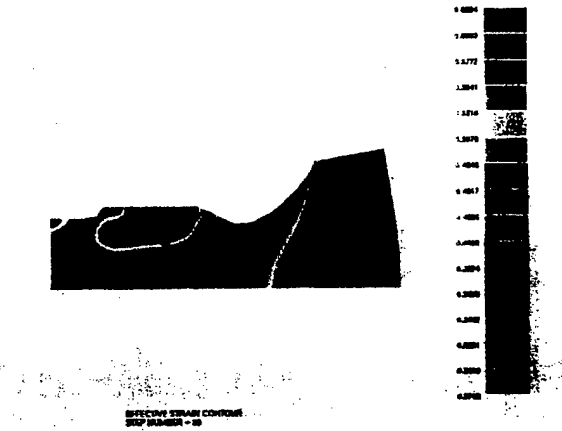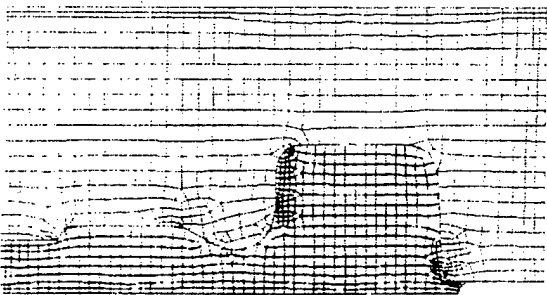
(a) Cost function used for optimization.

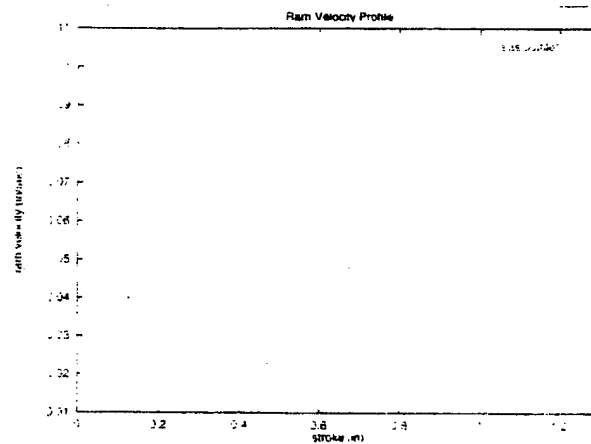(b) Weighing function, W, at a specific stroke
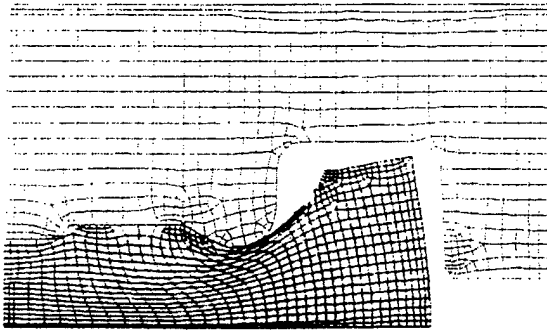
(c) Deformed geometry at 50% stroke

(d) Adaptively determined regions to be controlled (red and purple not controlled)

(e) Final deformed geometry

(f) Optimal ram velocity contour

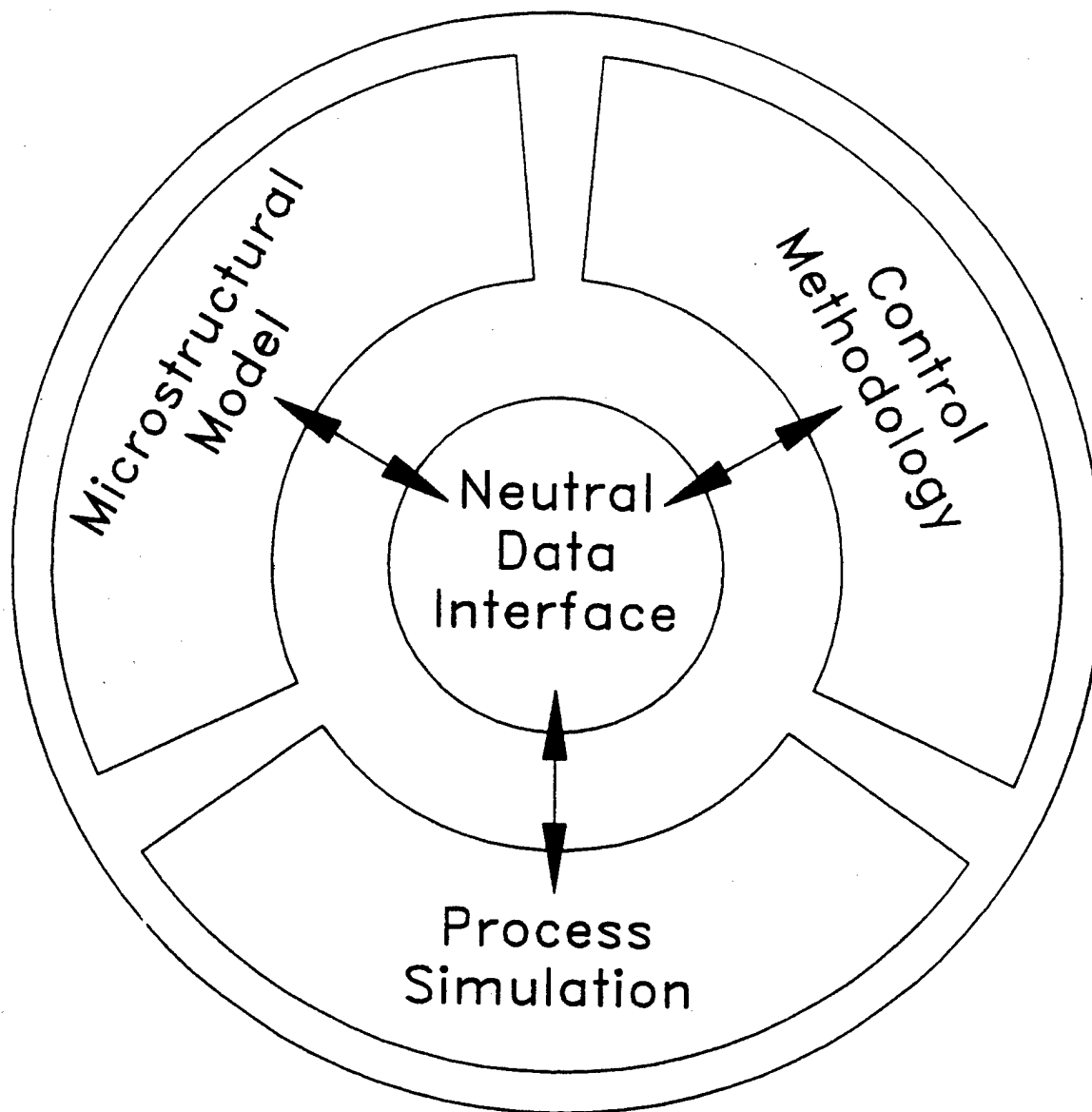Figure 7. Cost Function Based Controller for Disk Forging Process.

Figure 8. Neutral Data Interface Schematic.

11

The needs for the control and optimization modules are driven by the functions that a designer needs to perform. A list of user function versus information required is given in Figure 9. Note that for each function the information provided must be point tracked. Or in other words, given a desired starting closed region at a selected stage within the deformation, the neutral data interface will transfer information forward or backward tracking in deformation via interpolation across the remeshes and provide the required information in the succinct manner. An example of tracked regions is shown in Figure 10.

An additional function of the neutral data interface will be to return the cost function information directly from the process solver so as to permit a semi-black box type usage. Note that the neutral data interface tasks are not deemed to be difficult in their nature, but they are essential to be performed in order to eliminate the very large amount of drudgery involved in obtaining controlled/optimal solutions.

The neutral data interface itself will be developed to access the process solver results database and automatically perform the required transformations on the raw results data and output the final result in a succinct form. The interface needs to be developed with graphical support along with the supporting extracting and transformation software. Also considering that the nature of required information is highly specific and may need to be a hitherto undefined compound function of multiple parameters, the neutral data interface needs to have a generalized capability to compute the user defined functions and output them along with point tracking in a succinct single number numeric form whenever possible. In addition, the neutral data interface needs to support time or stroke dependent objective or cost function calculations. This development is a vital link in transferring this technology to the manufacturing industry since the users will not typically have the time or desire to perform detailed data transfer and calculation tasks in an error-free manner in order to correctly optimize the forming process.

User Functions	Needed Information
Ram Velocity Optimization	Strain rate distribution Deformation heating distribution Geometric quantities needed to perform weighted averages
Microstructural Control	Time integration of microstructural model equations
Fracture Control	Time integration of fracture criterion
Press Energy Optimization	Press energy expended as a function of time Cumulative stress power
Simultaneous Multistage Forming	Automated comparison of multiple workpiece results databases
Shrink Fit Pattern Optimization	Automated comparison of die stress results databases Automated superimposition of results for multiple shrink fit geometry stress solutions to obtain total stress values
Residual stress and Distortion Control	Residual stresses at desired locations Residual stresses transfer from as forged to machined geometry

Figure 9. Matrix of User Functions Versus Needed Information

13
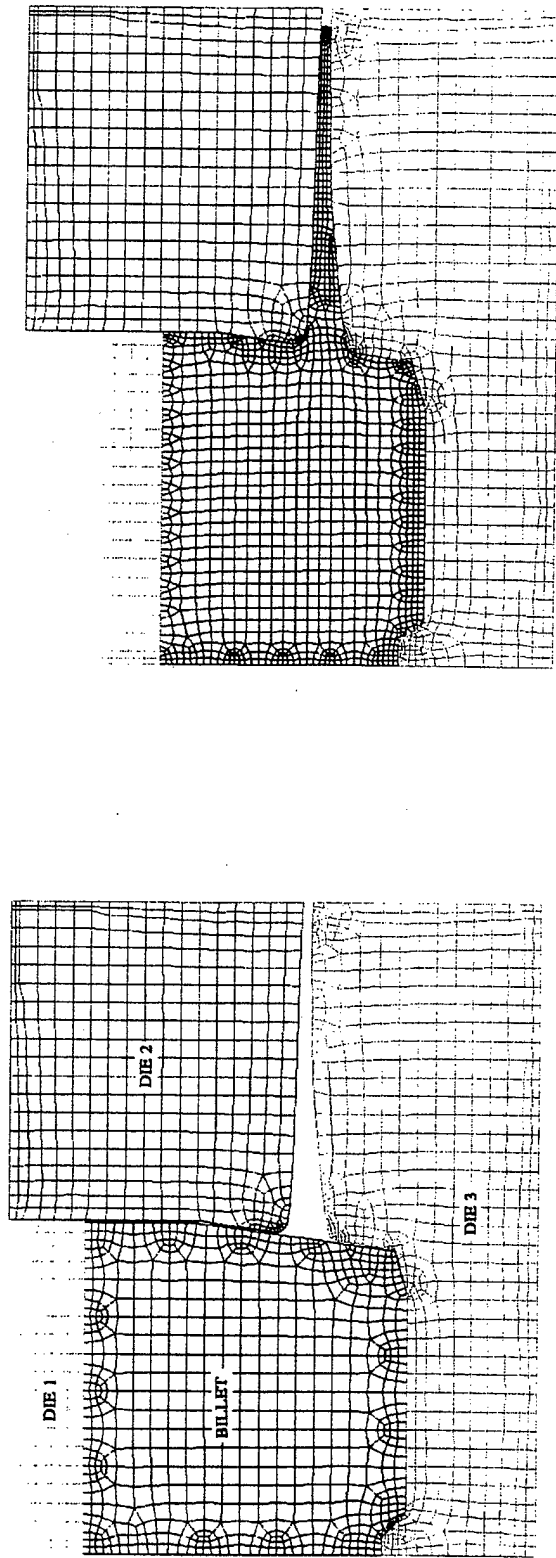
(a) Starting geometry

(b) Deformed geometry
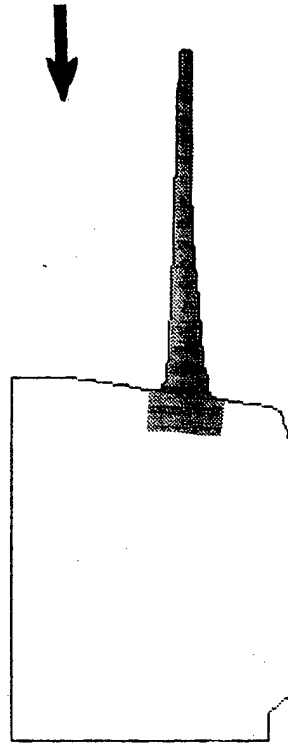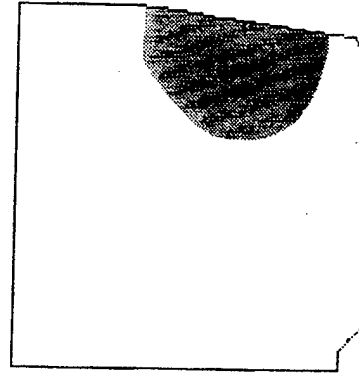
(c) Shaded area in the deformed geometry maps back to the shaded area in undeformed geometry.

Figure 10. Example of Point Tracked Region in Forged Disk.

4.0 RECOMMENDATIONS DERIVED FROM THE TECHNICAL MARKET SURVEY

The technology transfer for control and optimal design of forming processes will be performed in Phase II effort in active cooperation with the manufacturing industry by working with problems of direct interest to their specific sector. As a result, the technology transfer will involve multiple efforts which will run simultaneously in the Phase II effort. The specific nature and geometry of the problem considered will depend on the industry feedback and recommendations. It is anticipated that the effort will focus on the following specific objectives as described in Sections 4.1 to 4.4.

Note that the control and optimization techniques described below may be mixed and matched to the needs of the process. For example, at first, a variable ram velocity may be determined to control microstructural evolution during the forming process. This would be followed by determination of optimum quench parameters to minimize residual stresses and distortions.

4.1 FRACTURE CONTROL

This is essentially a variant of the open-loop control procedure developed in Phase I effort. The basic objective of this task is to determine a variable ram velocity such that the magnitude of the tensile stresses developed during the forming process is maintained below a critical limit which would result in occurrence of cracking. The same method may also be applied along with available phenomenological fracture models.

4.2 PRESS ENERGY INPUT OPTIMIZATION

This is a generalization of the variable ram velocity determination procedure for screw and hammer presses. For these energy bound presses, the evolution of the velocity profile depends on the sequence of expenditure of energy in deforming the workpiece. The total press energy is externally controllable rather than the ram velocity profile itself. The values of angular velocity for the screw press and drop height for the hammer will be considered for effecting the ram velocity during the forming process. This optimization will involve the following two steps. The first step will involve calculation of optimal material deformation trajectory based upon the material microstructural models only. The second step will involve optimization of press energy level so as to result in a minimum 'cost' in terms of loss of ideal deformation trajectory for the forming operation.

For a multiple stage operation where each stage is formed sequentially, this optimization procedure will involve variable press energy input calculation for each stage.

4.3 OPTIMAL RAM VELOCITY FOR SIMULTANEOUS MULTISTATION FORMING PRESS

The primary objective of this task will be to determine variable ram velocity for a press which performs multiple station forming simultaneously. This represents a tradeoff of improved

quality within individual forming stage for practical reasons of increased production. This effort will involve the following two major tasks:

1.   Utilize the material deformation trajectory control procedure via variable ram velocity for each individual stage separately. The calculation will account for the range of ram velocities permissible for the press considered. The total load of all simultaneously formed stages will be compared with the press capacity to determine feasibility in principle.

2.   The ram velocity profiles for independent forming of each stage will be scaled and added to obtain a linear combination. The optimization problem will then involve computation of optimal values of the scaling parameters to result in a minimum 'cost' in terms of loss of ideal forming conditions for the multiple stages considered.

4.4   RESIDUAL STRESS AND DISTORTION CONTROL

The basic objective of this task will be to develop quench parameters such that the residual stress magnitudes are small and the resulting distortions are within the desired tolerance level. This task is relevant across the forming industry for a wide range of components. This task will involve the two major steps as given below. The complex metallurgical transformations which occur during the sequence of operations given below will be phenomenologically accounted for to the extent feasible based upon availability of data.

1.   Perform simulation of the forming process in conformance with the specified process parameters.   The workpiece deformation will be computed using the elasto-viscoplasticity computations. Simulate the thermal history of the part through its heat treatment cycle and note the evolution of time versus temperature history for each point within the component.

2.   Simulate the quenching process. This process will be comprised of air and oil/water quench as required. For the oil/water quenching, the angle of dip for the components will be considered as a variable since the sequence of cooling is likely to influnce the distortion particularly in case of thin components. For each stage of the quenching process, utilize the temperature of the medium and its agitation level as the externally controllable process variables to minimize the residual stress and distortion levels.

16

5.0   <u>CLOSURE</u>

The technical accomplishments of this Phase I program are:

1.   Development of an open-loop control system for forging processes

2.   Development of specifications for a neutral data interface between process modeling, equipment model and microstructural models to facilitate effective control of the forming process.

3.   Development of optimal material deformation trajectories to attain the desired microstructure.

4.   Development of recommendations from the manufacturing industry for the most relvant forging process control needs.

For the technical effort performed under this Phase I program, UES, Inc. was the prime contractor with AES, Inc. as a subcontractor. The Phase II effort will focus on implementation of the recommendations of the manufacturing industry for the different aspects of the forging process control as well as its technology transfer.

APPENDIX A

OPEN-LOOP CONTROL OF A HOT-FORMING PROCESS

By

Jordan M. Berg
USAF Wright Laboratories
Wright-Patterson AFB, OH 45433

Anil B. Chaudhary
UES, Inc.
4401 Dayton-Xenia Road
Dayton, OH 45432-1894

James C. Malas III
USAF Wright Laboratories
Wright Patterson AFB, Ohio 45433

Open-loop control of a hot-forming process

Jordan M. Berg
USAF Wright Laboratories, WPAFB, Ohio, USA

Anil Chaudhary
UES, Inc., Dayton, Ohio, USA

James C. Malas III
USAF Wright Laboratories, WPAFB, Ohio, USA

ABSTRACT: A simulation study is performed to show that nonlinear finite-element process models can be integrated with material microstructural evolution equations ito develop an automated tool for the design of ram velocity profiles. The example presented is an isothermal forging of a complex disk shape from a γ phase titanium-aluminide alloy. The objective is to choose a ram velocity profile that maintains a desirable strain rate throughout the billet. For an arbitrarily complex given die and workpiece geometry, this objective is typically unattainable An acceptable compromise is obtained by controlling the strain rate only in regions of the billet where the material is undergoing microstructural transformation. The techniques developed in this paper can be generalized to a variety of design goals and forging parameters.

1 INTRODUCTION

Designing a complex forging based on repeated trials consumes valuable time and requires expensive equipment. The availability of reliable commercial nonlinear finite-element algorithms allows much of the iteration to be shifted to a computer, cutting costs. However, the process is still trial-and-error (now on a computer), and requires frequent input from a designer. This interaction can be further reduced. Once the designer has specified desired properties of the finished piece, and has indicated which process parameters are constrained and which can be freely varied, the search can be conducted automatically. The designer is freed from a tedious task, and productivity is increased. These gains are most dramatic when combined with automatic remeshing. With automatic remeshing now available for 3-D forgings, these techniques can be used on any part.

For the current effort, an isothermal forging is first expressed in an open-loop optimal control formulation. The design objective is written as a cost function to be minimized, subject to such constraints as are required. A wide variety of techniques exist to solve such problems. The choice of approach is strongly dependent on the specific form of the microstructural evolution equations. For the present case, the evolution equation for the fraction of material transformed is strongly dependent on effective strain, and only weakly dependent on strain rate. The equation describing the average transformed grain size has the opposite character.

This paper presents simulation results for this sample case. An axisymmetric cupped disk is to be formed from a TiAl alloy. The starting microstructure is specified. The process model is a nonlinear finite-element code. Die and preform shapes are fixed, and the forging is to be accomplished in a single step. The goal is to achieve the required shape, while transforming as much of the material as possible into a desired final microstructure. The variable control parameter to be optimized is the ram velocity.

2 DESIGN OBJECTIVES

The forging has two critical aspects. The first is shaping the billet. The die and preform geometries are specified. They are shown in Fig. 2.1. Figure 2.2 shows the situation when the ram has reached its full stroke of 2.8 in. Attaining the desired shape is a strict constraint, which is considered to have been exactly achieved when the ram reaches full stroke.

The second aspect, on which this study concentrates, is transforming the billet microstructure. The material considered here is Ti-48Al-2V. This material, in its γ phase, has high yield strength at elevated temperatures, making it extremely useful in aerospace applications. The γ alloy has a low ductility, however, and so is difficult to form and too brittle for many applications. The cast and hipped material has a lamellar structure, with alternating α_2 and γ layers. During deformation, the lamellar structure is transformed to one of equiaxed grains of pure γ and pure α_2 phase material (dynamic spheroidization). If the grains are small, then the material combines high temperature

strength with improved ductility. ..e size of the spheroidized grains can be controlled using the deformation parameters. The design goal considered in this paper is achieving maximum spheroidization, and a minimal grain size.
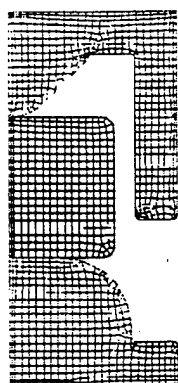

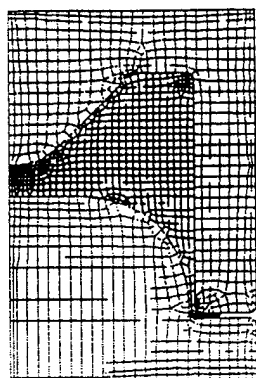Figure 2.1. Undeformed forging geometry.

Figure 2.2. Forging geometry at full stroke.

Guillard (1994) has given desirable process parameters for isothermal, constant strain rate, compression. Guillard's work also indentifies a processing window in the strain-strain rate-temperature space to ensure material stability, and gives microstructural evolution equations that describe the average spheroidizeded grain size, and the fraction of material spheroidized, in terms of the strain, strain rate, and temperature.

The present work jointly utilizes the strain, strain rate, and temperature information output from the process simulation model in order to automatically arrive at the optimal ram velocity. Figure 2.3 shows the processing map at a strain of 0.7. The light gray region represents a likely processing window based on stability considerations, as discussed in Malas & Seetheraman (1992). The processing target can be further refined, using the techniques of optimal control theory, following the method of Malas, Irwin, and Grandhi (1993). The result, calculated by Frazier (1994) is the point indicated in Fig. 2.3. That

is, the objective is to ..ep the material as close as possible to a strain rate of 0.3 1/min, at a temperature of 1100 C throughout the entire forging. The forging is assumed to be isothermal, so achieving the desired strain rate is the only objective.
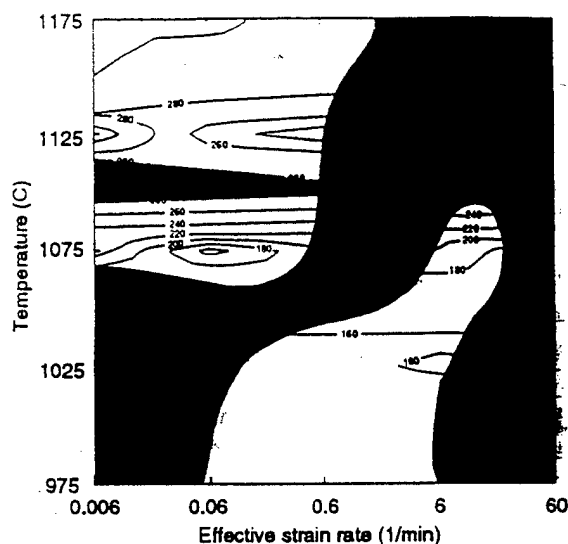

Fig 2.3. Deformation processing map at effective strain of 0.7. Unstable regions are blacked out, activation energy is background, processing window is shaded.

3 PROCESS MODEL

The macroscopic aspects of the forging are modeled using widely available commercial forming software, *Antares* (UES, Inc. 1993). This software uses a standard nonlinear implicit iterative finite element based computational strategy to perform forging analysis. The workpiece material is modeled as rigid-viscoplastic and a shear friction constitutive law is used for characterization of die-workpiece interface behavior.

4 NUMERICAL OPTIMIZATION

Given the control objective of obtaining a final forged microstructure that is completely spheroidized, and of the desired grain size, it is also necessary that the material stay within the pre-specified processing window. Since the progress of the forging is parameterized by the ram stroke, and the initial microstructure and the desired final microstructure is specified, it is viewed as a fixed end-point problem, where the cost function depends only on the final state, but the path is subject to inequality constraints. This approach requires that the microstructural evolution equations be integrated into the finite-element package. At the time this analysis was performed, that had not been done. Since then, it has been accomplished, and that software was used to evaluate the results of this study. However, a different method was used for the optimization.

As discussed in the previous section, the objective of the forging is to keep the strain rate at 0.3 1/min, at the temperature at 1100 C throughout the entire billet and at all times. In terms of the finite element process model, this means keeping every element in the billet at the optimal strain rate at every stroke increment. Except for an idealized frictonless upsetting, this will typically be impossible. Strain rates will vary across the billet, and most regions will be either above or below the desired value. The problem then becomes to achieve the minimum deviation from the desired process window, across the workpiece and throughout the stroke.

The best way to write the cost function for this problem is as the sum of the squares of the strain rate error for each element. At each step, then, the ram velocity that minimized this cost function would be determined. Another reasonable approach is to find the ram velocity at each step that drives the average strain rate across the billet to the desired value. These two formulations may seem similar, but they are quite different. The first is more physically meaningful for this problem. The second is far preferable numerically. The two will coincide when the strain rate distribution across the billet is uniform, otherwise the first method gives a lower value. It is important to note that if the strain rate variations throughout the billet is large, then neither technique will give good results. On the other hand, if the strain rate variations are small, then either method will work well. So if some means are found to reduce the strain rate variation, the approach with better numerical properties can be used, and it will give a good result.

The distribution of strain rates throughout the workpiece is strongly affected by the die/billet geometry. Once the geometry has been set, as is the case in this study, the designer has little further influence. However, the strain rate variation can be effectively reduced by only considering a portion of the billet. This is justified on the following grounds: The material is not transforming evenly. Some parts of the billet are nearly rigid, and are not transforming at all, while others may have been totally transformed already. Therefore it is possible to weight each point in the billet, based on the microstructural evolution equation describing its fraction transformed. That calculation is now discussed in detail.

Let $S(\varepsilon,\dot{\varepsilon},T)$ be the microstructural evolution equation describing the fraction of material transformed (spheroidized, in this case). The weighting of a piece of material will be proportional to the amount of material transforming during this stroke increment. That is,

$$W(\varepsilon,\dot{\varepsilon},T) = K\frac{dS}{dX}\Delta X \qquad (4.1a)$$

$$\approx K\frac{\partial S}{\partial\varepsilon}\frac{\Delta\varepsilon}{\Delta t}\frac{\Delta t}{\Delta X} \qquad (4.1b)$$

$$\approx K\frac{\partial S}{\partial\varepsilon}V_{ram} \qquad (4.1c)$$

$$\approx K'\frac{\partial S}{\partial\varepsilon}\dot{\varepsilon} \qquad (4.1d)$$

where X is stroke, and t is time. This approximation assumes that the fraction spheroidized changes due to changes in strain only, and neglects effects due to changes in strain rate, and temperature. Temperature variations are not considered because of the isothermal assumption. Strain rate effects are considered to be small based on the character of the microstructural evolution equations. Also note that the experimental data underlying the expression for S are for constant strain rate compressions. As a result, the level of accuracy is difficult to determine for complex strain rate paths, without further extensive experimentation.

The microstructural evolution equation for S is as follows (Rack, 1994):

$$S(\varepsilon,\dot{\varepsilon},T) = 2061.38 + 7.017\log\dot{\varepsilon} - 3.7908\,T + 56.84\,\varepsilon + 0.001776\,T^2 - 12.52\,\varepsilon^2 \qquad (4.2)$$

where T is the temperature specified in degrees C, log is base 10, and time is in seconds. It is understood that when the strain exceeds 2.27, the fraction transformed is one. So,

$$\frac{\partial S}{\partial\varepsilon}\dot{\varepsilon} = (56.84 - 25.04\,\varepsilon)\,\dot{\varepsilon} \qquad (4.3)$$

and,

$$W(\varepsilon,\dot{\varepsilon},T) =$$

$$\begin{cases} (56.84 - 25.04\,\varepsilon)\,\dot{\varepsilon} & 0 \le \varepsilon \le 2.227 \\ 0 & 2.227 \le \varepsilon \end{cases} \qquad (4.4)$$

The microstructure model derived by Guillard is based on a curve fit to experimental data. That fit is strictly valid only in the region,

$$0.35 \le \varepsilon \le 2.03 \qquad (4.5a)$$

$$10^{-4}\,s^{-1} \le \dot{\varepsilon} \le 10^{-1}\,s^{-1} \qquad (4.5b)$$

$$1058\,C \le T \le 1142\,C \qquad (4.5c)$$

Note that this is particularly restrictive at the low end of the strain scale. Most forgings start with the billet material at close to zero strain. Furthermore, the weighting is at a maximum when the strain is zero, so these regions are simultaneously poorly modeled, and extremely important. This is an undesirable situation, but for now—pending the development of more suitable models—unavoidable.

The weighting function can be used in either the least squared error, or the mean strain rate, formulation. The remainder of this paper considers only the mean strain rate formulation. The cost function to be minimized is,

$$J = (\dot{\varepsilon}_{des} - \dot{\varepsilon}_{av})^2 \qquad (4.6)$$

where $\dot{\varepsilon}_{av}$ is a weighted average strain rate, given by

$$\dot{\varepsilon}_{av} = \frac{\sum W_i^n \dot{\varepsilon}_i}{\sum W_i^n} \qquad (4.7)$$

The computational advantage of this cost function springs from the fact that the weighted average strain rate can almost always be set to any desired value, by varying the ram velocity. Thus the problem of minimizing J reduces to the problem of finding the root of $\dot{\varepsilon}_{des} - \dot{\varepsilon}_{av} = 0$. The root finding problem is easy because Eqn. (4.7) is a monotonically increasing function of ram velocity, with a guaranteed zero crossing. The exponent, n, is a design parameter that allows the most rapidly spheroidizing regions of the material to be most heavily weighted. Note in particular that as n increases, the volume of material being actively controlled will decrease, and the strain rate in those regions will be very close to the target strain rate. When n is zero, the result is the unweighted average strain rate in the billet.

The root finding algorithm begins by bracketing the zero. Once bracketed, it switches to a general purpose routine called Brent's method (Press, et al. 1986). Brent's method switches between parabolic interpolation and bisection, depending on whether the parabolic fit is good. When the interval is within an acceptable tolerance the routine terminates. Figure 4.1 shows how Brent's method is integrated with *Antares*.
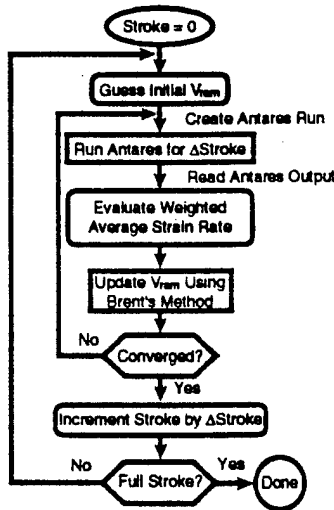

Figure 4.1. General scheme for optimizing ram velocity via Brent's method.

Note that Brent's method does not use derivative information. In principle, the derivatives can be obtained from the process simulation code. However, the total effort required to obtain such information in a succinct form is deemed to be extremely large, and therefore was not performed as part of this study.

5 EVALUATION MODEL

Once the cost function has been selected, and the optimizing ram velocity profile found, the result

must be evaluated. . this point all simplifying assumptions should be dropped. The ideal test of the optimal ram velocity would be an actual forging, but this was not an available option. The main difficulty in evaluating the result of the optimization in simulation is that the microstructural evolution equations must be integrated into the finite-element simulation. As has been mentioned, these equations were derived for constant strain rate compression tests, so the limitations on their use in complex forging situations needs to be duly considered.

The microstructural evolution equations are Eqn (4.2), given previously, and (Rack, 1994):

$$g(\varepsilon, \dot{\varepsilon}, T) = 248.22 + 142.97 \log \dot{\varepsilon} - 0.1284\, T -$$

$$59.82\, \varepsilon + 8.77 \log^2 \dot{\varepsilon} + 7\, \varepsilon^2 - 0.0833\, T \log \dot{\varepsilon} -$$

$$15.833\, \varepsilon \log \dot{\varepsilon} \qquad (5.1)$$

where g is the average transformed grain size, in microns, T is the temperature specified in degrees C, log is base 10, and time is in seconds. Again, the restrictions (4.5) apply to Eqn. (5.1).

As in the case of the weighting function, the low strain region is unavoidable, and critically important. There is, however, no alternative at the moment, short of actual experiments.

Equations (4.2) and (5.1) represent solutions to microstructural state equations for isothermal, constant strain rate compressions. What is required for the purposes of the evaluation model are equations governing behavior for nonconstant strain rate compressions, that is, expressions for $dS/dt(\varepsilon, \dot{\varepsilon}, T)$ and $dg/dt(\varepsilon, \dot{\varepsilon}, T)$.

$$\frac{dS}{dt}(\varepsilon, \dot{\varepsilon}, T) = \frac{\partial S}{\partial \varepsilon}\frac{\partial \varepsilon}{\partial t} + \frac{\partial S}{\partial \dot{\varepsilon}}\frac{\partial \dot{\varepsilon}}{\partial t} + \frac{\partial S}{\partial T}\frac{\partial T}{\partial t} \qquad (5.2a)$$

$$\approx \frac{\partial S}{\partial \varepsilon}\dot{\varepsilon} \qquad (5.2b)$$

$$\approx (56.84 - 25.04\,\varepsilon)\,\dot{\varepsilon} \qquad (5.2c)$$

$$\frac{dg}{dt}(\varepsilon, \dot{\varepsilon}, T) = \frac{\partial g}{\partial \varepsilon}\frac{\partial \varepsilon}{\partial t} + \frac{\partial g}{\partial \dot{\varepsilon}}\frac{\partial \dot{\varepsilon}}{\partial t} + \frac{\partial g}{\partial T}\frac{\partial T}{\partial t} \qquad (5.3a)$$

$$\approx \frac{\partial g}{\partial \varepsilon}\dot{\varepsilon} \qquad (5.3b)$$

$$\approx (-59.82 + 14\,\varepsilon - 15.833 \log \dot{\varepsilon})\,\dot{\varepsilon} \qquad (5.3c)$$

Neglecting the temperature effects is justified, if the forging is truly isothermal. Neglecting the strain rate term is justified if the strain rate varies slowly. It is preferable to include these effects, particularly for evaluation, but the spatial distributions of time derivatives of strain rate and temperature across the billet domain are not easily available from the process solver, due to the multiple remeshings performed throuhout the progression of the forging. Furthermore, the microstructural evolution equations

were derived for isothermal and constant strain rate conditions, so they are best used when these terms are small. With these restrictions understood, (5.2c) and (5.3c) are appended to the other state equations in the process solver. The final microstructure distribution can be displayed using a graphical post-processor.

Ideally the evaluation model would be improved through a better understanding of the microstructural evolution dynamics, and used directly for optimization. It would seem that the biggest payoffs for both analysis and synthesis of forgings would come from developing such codes.

6 RESULTS

The algorithm described in the preceding section was applied, for values of n equal to 0, 1, 2, 4, and 8. The resulting ram velocity profiles are shown in Fig. 6.1. Also shown in Fig. 6.1 is a linear velocity-stroke curve. This curve is obtained by modeling the forging as a simple frictionless upsetting, and using the ram velocity that gives the target strain rate.
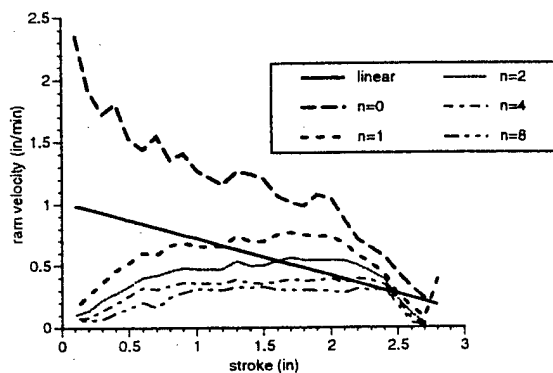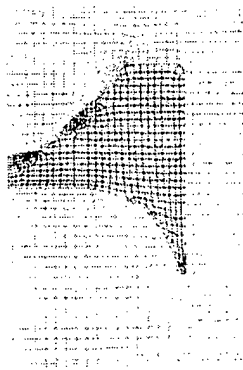

Fig. 6.1. Ram velocity profiles.

Fig. 6.2. Geometry at stroke of 2.6 in.

The character of each solution can be illustrated by considering the strain rate distributions at a particular stroke. Figure 6.2 shows the geometry at a stroke of 2.6 in. Figure 6.3 shows the effective strain distribution at this stroke. The results for $n = 8$ are shown, but the effective strain is largely independent of the ram velocity profile. Figures 6.5 and 6.6 compare the strain rates in the billet at this stroke for the linear solution, and the case $n = 4$.

The results show the effectiveness of the algorithm. Because only a small portion of the material is transforming at the end of the forging— that in the rim of the "bowl"—the velocity profiles that do not explicitly account for the microstructural evolution do not adequately control the process. In particular, the unweighted average strain rate objective, and the linear profile both produce unacceptably high strain rates in the transforming region. Review of Fig. 2.3 shows that the material will be in the unstable region of the processing map. The result will be flow localization or cracking.

On the other hand, the weighted strain rate objectives do significantly better. The cases of $n = 4$, and $n = 8$, both keep the transforming material within the process window. The rest of the billet will be out of the window, with strain rates orders of magnitude below the target. This corresponds to undesirable transformation mechanisms. But because very little of this material actually transforms, the quality of the end product is not significantly affected. Finally, Fig. 6.6 and 6.7 show the average transformed grain size, and fraction transformed, respectively, predicted for the case $n = 4$. The final microstructure is not very good. Since the ram velocity is, in a meaningful sense, optimal, further improvements will require redesign of the dies and/or preform.
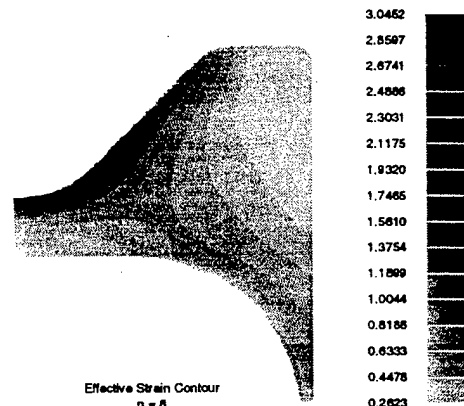

Fig. 6.3. Effective strain distribution at a stroke of 2.6 in, for $n = 8$ velocity-stroke curve.
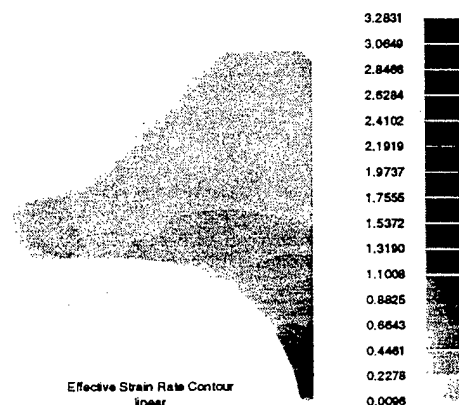

Fig. 6.4. Effective strain rate distribution at stroke of 2.6 in, for linear velocity-stroke profile.
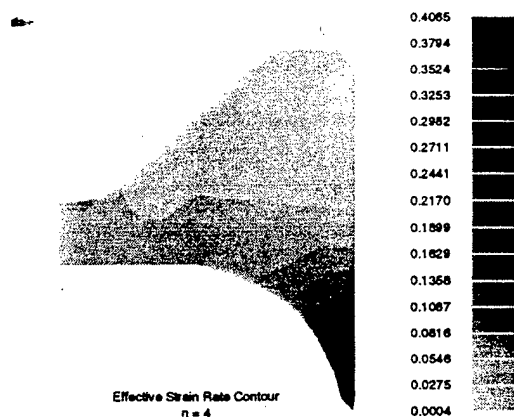
23

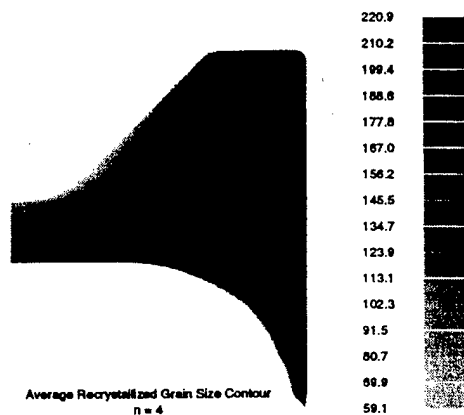Fig. 6.5. Effective strain rate distribution at stroke of 2.6 in for case $n = 4$.

Fig. 6.6. Spheroidized grain size distribution at stroke of 2.6 in for case $n = 4$.
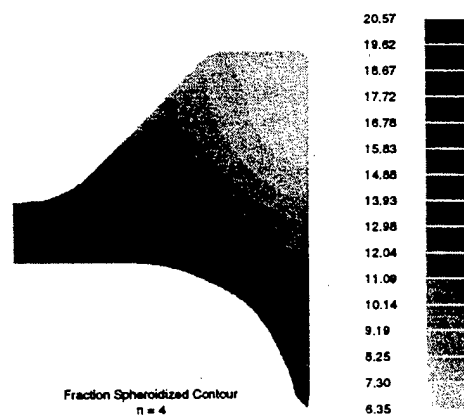

Fig. 6.7. Fraction recrystallized distribution at stroke of 2.6 in for case $n = 4$.

7 CONCLUSIONS

The integration of microstructural models and nonlinear finite element simulations adds a new tool to aid the forging process designer. This tool shows great promise in simulation studies. Once die and preform geometries are selected, the algorithm described generates ram velocity profiles that optimally produce a desired microstructure. The key innovation is a weighting function that concentrates on only those regions with a transforming microstructure. The degree to which these regions are emphasized is controlled by a weighting exponent. This exponent can be varied as a design parameter. The use of microstructural evolution equations incorporated into the finite element process model provides a very useful analysis tool for predicting the properties of the finished part.

REFERENCES

Frazier, W.G. 1994. Personal communication.

Guillard, S. 1994. *High Temperature Micro-Morphological Stability of the ($\alpha_2 + \gamma$) Lamellar Structure in Titanium Aluminides,* Ph.D. Thesis, Materials Science and Engineering Dept., Clemson University.

Malas, J.C. and V. Seetharaman 1992. Using Material Behavior Models to Develop Process Control Strategies, *JOM*, 44:8–13.

Malas, J.C. R.D. Irwin, and R.V. Grandhi 1993. An Innovative Strategy for Open Loop Control of Hot Deformation Process, *Journal of Materials Engineering and Performance*, 2:703–714.

Press, W.H., B.P. Flannery, S.A. Teukolsky, W.T. Vetterling 1986. *Numerical Recipes: The Art of Scientific Computing*: 251-254. Cambridge, Cambridge University Press.

Rack, H. 1994. Personal communication.

UES, Inc. 1993. *Antares User's Manual Version 3.0*, Dayton OH.

APPENDIX B

DETERMINATION OF OPTIMAL MATERIALS DEFORMATION TRAJECTORIES

By

Dennis Irwin and Enrique Medina

Austral Engineering and Software, Inc.
9 Pleasantview Drive
Athens, Ohio 45701

1.0 Introduction

This report documents AES efforts on the Phase I SBIR "Intelligent Control Systems for Hot Forming and Extrusion". These efforts were organized into the following tasks: (1) define parts of the neutral data interface, (2) provide microstructural modeling code, (3) provide microstructural trajectory optimization code, (4) investigate enhanced node or location choice for ram velocity optimization, and (5) support UES in the communication of team capabilities to the forming industry consortium to be organized under Phase I.

All tasks were successfully performed by AES personnel. However, rather soon after the initiation of the subcontract, it became clear that the planned approaches for Task 4 were not feasible. Therefore, a state of the art graphical interface for using the results of Task 2 and Task 3 efforts was developed. This effort is also documented in the following.

The report is organized in seven sections, of which this introduction is the first, and two appendices. The second section discusses the analytical aspects of the microstructural modeling approach. The third section outlines the algorithm and approach for microstructural trajectory optimization and the fourth section contains details of the code developed for microstructural modeling and microstructural trajectory optimization, as well as details of the graphical user interface. The fifth section contains details of the data formats required for the neutral data interface. The sixth section discusses the topic of selection of locations for trajectory control. Section seven presents some conclusions regarding the Phase I effort and some recommendations for future work. Appendix A describes the material model used to test the microstructural trajectory optimization algorithm. Finally, Appendix B gives some information about the three-dimensional plotting package used by the software for comparisons between models and data.

2.0 Microstructural Modeling

The initial step in the application of control methodologies to hot forming processes consists of obtaining reliable models that describe material behavior during the deformation process.

The current microstructural modeling technique is based on ordinary least squares. Enhancements to the basic least squares algorithm (constrained least squares, interpolation approaches, etc.) will likely be necessary to achieve a general modeling module; however, they are not currently implemented. Also, the current models do not include any dynamic effects since the available compression test data are completely static in nature. However, the neutral data interface file formats contain provisions for dynamic models of spheroidization and/or recrystallization.

The same algorithm is used to generate models for flow stress, grain size, and fraction spheroidized. The following discussion is for generation of flow stress models, but it should be realized that similar developments are true for fraction spheroidized and grain size.

2

Since it is difficult to envision the same microstructural mechanisms being present for a wide range of materials, it was decided that polynomial models would be used to describe the material microstructural behavior. The polynomial models are third degree in three variables:

$$
\begin{aligned}
\sigma(\varepsilon,\dot{\varepsilon},T) = {} & a_1 + a_2\varepsilon + a_3\theta + a_4\beta + a_5\varepsilon\theta + a_6\varepsilon\beta + a_7\theta\beta \\
& + a_8\varepsilon^2 + a_9\theta^2 + a_{10}\beta^2 + a_{11}\theta\varepsilon^2 + a_{12}\beta\varepsilon^2 + a_{13}\varepsilon\theta^2 \\
& + a_{14}\theta^2\beta + a_{15}\varepsilon\beta^2 + a_{16}\beta^2\theta + a_{17}\varepsilon^3 + a_{18}\theta^3 + a_{19}\beta^3 + a_{20}\varepsilon\theta\beta \ ,
\end{aligned}
\tag{1}
$$

where $\theta = 1/T$, $\beta = \log_{10}(\dot{\varepsilon})$, ε is the strain, $\dot{\varepsilon}$ is the strain rate, and T is temperature. In the modeling paradigm, the coefficients (a_i's) are the unknown quantities and there is a distinct equation for each measured value of flow stress that can be formed for each set of strains, strain rates, and temperatures. For example, at the ith temperature, the jth strain rate, and the kth strain, and from the measured flow stress at this condition:

$$
\begin{aligned}
\sigma_{i,j,k}(\varepsilon_k,\dot{\varepsilon}_j,T_i) = {} & a_1 + a_2\varepsilon_k + a_3\theta_i + a_4\beta_j + a_5\varepsilon_k\theta_i + a_6\varepsilon_k\beta_j + a_7\theta\beta_j \\
& + a_8\varepsilon_k^2 + a_9\theta_i^2 + a_{10}\beta_j^2 + a_{11}\theta\varepsilon_k^2 + a_{12}\beta_j\varepsilon_k^2 + a_{13}\varepsilon_k\theta_i^2 \\
& + a_{14}\theta_i^2\beta_j + a_{15}\varepsilon_k\beta_j^2 + a_{16}\beta_j^2\theta_i + a_{17}\varepsilon_k^3 + a_{18}\theta_i^3 + a_{19}\beta_j^3 + a_{20}\varepsilon_k\beta_j\theta_i \ .
\end{aligned}
\tag{2}
$$

The equations for all of the test conditions available form a set of linear equations with the a_i's as the unknowns. A least squares solution to these equations is sought using a singular value decomposition (SVD) based pseudo-inverse approach. Some comments on the results of this approach applied to a TiAl alloy are given in Appendix A, while a three dimensional plot that compares a model of flow stress obtained by this method to the original data is presented in one of the screen dumps of Section 4.

3.0 Trajectory Optimization

In this work, an optimization algorithm is used to obtain a strain rate trajectory that will take the material model microstructural and workability conditions from given initial states to desired final states. The theory on which the algorithm is based and the algorithm itself are described in this section.

A fourth order state space model is used to represent the material dynamics during deformation. Percent spheroidization s, temperature T, strain ε, and grain size d are chosen as state variables, i.e., the state vector is defined as

$$
x(t) = \begin{bmatrix} s(t) \\ T(t) \\ \varepsilon(t) \\ d(t) \end{bmatrix} .
\tag{3}
$$

The dynamic behavior of the material is described by the state equation

$$
\dot{x} = f(x(t),u(t)), \qquad x(0) = x_0 \in \mathbf{R}^4,
\tag{4}
$$

where $u(t)$ is the strain rate, which is considered the input to the system, x_0 is the vector of initial states, $\dot{x}(t)$ is the time derivative of $x(t)$, and f is a function that relates $\dot{x}(t)$ to $x(t)$ and $u(t)$.

3

The trajectory optimization problem can be stated as follows: Given the system described in Equation 4, find the strain rate trajectory $u(t)$ that minimizes the cost function

$$J = h(x(t_f),t_f) + \int_0^{t_f} g(x(t),u(t))\, dt \quad , \tag{5}$$

where t_f is the final time, and functions h and g define the contribution of the final state, final time, state trajectory, and control trajectories to the cost function. If g and h are selected appropriately, minimization of J produces a control trajectory that takes the states to the desired final values while maintaining acceptable state and control trajectories. In practice, there are tradeoffs between the achievement of the various desired goals.

The standard approach to finding necessary conditions for the solution to this problem is based upon augmenting the process constraints (the material behavior model of Equation 4) to the cost functional J through the use of Lagrange multipliers and then seeking to satisfy the necessary conditions for constrained minimization. The augmented functional is given by

$$J_a = h(x(t_f),t_f) + \int_0^{t_f} \Big[g(x(t),u(t)) + p^T(t)(\dot{x}(t) - f(x(t),u(t)))\Big]\, dt \quad , \tag{6}$$

where p is the vector of Lagrange multipliers.

It is customary in the approach to obtaining the necessary conditions to define the function

$$H = g + p^T f \, , \tag{7}$$

which is usually referred to as the Hamiltonian. The time dependence has been dropped for brevity.

It can be shown that the necessary conditions in order for $u(t)$ to minimize J are (Kirk, 1970)

$$\dot{p}^T = -\frac{\partial H}{\partial x} = -\left(\frac{\partial g}{\partial x} + p^T\frac{\partial f}{\partial x}\right) \quad , \tag{8}$$

$$\dot{x} = f \quad , \tag{9}$$

$$\frac{\partial H}{\partial u} = \frac{\partial g}{\partial u} + p^T\frac{\partial f}{\partial u} = 0 \, , \tag{10}$$

4

$$x(0) = x_0 , \tag{11}$$

and

$$p(t_f) = \frac{\partial h}{\partial x}\big(x(t_f), t_f\big) , \tag{12}$$

where $\frac{\partial g}{\partial x}$ is the gradient of g and $\frac{\partial f}{\partial x}$ is the Jacobian matrix of f. It is emphasized that these conditions are only necessary conditions for optimality and they do not constitute a solution approach by themselves.

The most straightforward solution approach consists of seeking an iterative algorithm that possesses the property that each successive iterate is closer to satisfying the above conditions than the previous iterate. The following algorithm is one such approach. It is based on direct application of variational principles.

Given an initial guess $u(t)^{(0)}$ for the optimal control trajectory, calculate a variation on $u(t)$, $\delta u^{(0)}$, such that $u^{(0)} + \delta u^{(0)}$ decreases the value of $J(u)$, i.e.,

$$J(u^{(0)} + \delta u^{(0)}) < J(u^{(0)}) . \tag{13}$$

Repeat this process until no further decrease in J is obtainable.

The basis of the calculation of δu at each iteration is the notion of the first variation of a functional. It can be shown that if equations 8, 9, 11 and 12 are satisfied, which is easy to ensure, then the first variation of $J_{\bullet}$ is

$$\delta J_{\bullet} = \int_0^{t_f} \frac{\partial H}{\partial u} \, \delta u \, dt . \tag{14}$$

A clear choice for δu in order for $\delta J_{\bullet} < 0$ to be satisfied becomes

$$\delta u = - \frac{\partial H}{\partial u} . \tag{15}$$

Since this is only a first order variation, the range over which this variation is accurate is limited. Therefore, it is necessary to select a "step length" α to ensure that

$$J(u + \alpha u) < J(u) \tag{16}$$

by a sufficient amount.

Another difficulty is the phenomenon of slow convergence that is associated with repeatedly using this correction iteration after iteration. This slow convergence is due to the lack of information concerning the curvature of the functional. One approach to alleviating some of this difficulty is to estimate curvature information using the results of previous iterations. Although there are many formulas for doing this for problems in finite dimensional spaces, only a few are suitable for extension to problems on infinite dimensional spaces such as the optimal control problem. The following formula for calculating a better correction is termed a "self-scaled, memoryless quasi-Newton update" (Frazier, 1994).

5

$$d_{k+1} = \frac{\langle \Delta u, \Delta(\nabla_u H)\rangle}{\left\|\Delta(\nabla_u H)\right\|_2^2} \nabla_u H$$

$$+ \left[\frac{2\langle \Delta u, \nabla_u H\rangle}{\langle \Delta u, \Delta(\nabla_u H)\rangle} - \frac{\langle \Delta(\nabla_u H), \nabla_u H\rangle}{\left\|\Delta(\nabla_u H)\right\|_2^2} \right] \Delta u \qquad (17)$$

$$- \frac{\langle \Delta u, \nabla_u H\rangle}{\left\|\Delta(\nabla_u H)\right\|_2^2} \Delta(\nabla_u H) \ .$$

In this formula, d_{k+1} is the directional vector of change for the input trajectory $u(t)$. The correction to $u(t)$ from step k to step $k+1$ of the algorithm is given by

$$\Delta u = u_{k+1} - u_k = \tau_k d_k \ , \qquad (18)$$

where τ_k is the step length at step k of the algorithm. The rest of the notation is given by

$$\nabla_u H = \left(\frac{\partial H}{\partial u}\right)_k \ , \qquad (19)$$

$$\Delta(\nabla_u H) = \nabla_u H_{k+1} - \nabla_u H_k \ , \qquad (20)$$

$$\langle f_1, f_2\rangle = \int_0^{t_f} f_1 f_2 \, dt \ , \qquad (21)$$

and

$$\| f \|_2^2 = \langle f, f\rangle \ . \qquad (22)$$

The derivation of formula 17 is not given here, however it is based upon the standard BFGS update restricted to using only information from one previous iteration combined with a self-scaling strategy suggested by Luenberger (1984) for quasi-Newton type algorithms. See the text by Luenberger for a good introduction to quasi-Newton methods applied to finite dimensional spaces. Equation 21 is simply the inner product on the interval $[0, t_f]$.

The determination of the step length is based on satisfying a sufficient decrease in the cost as well as a sufficient reduction of the directional derivative (Wolfe's test, Luenberger,(1984)). Overall algorithm convergence is measured by four criteria. In order to ensure that the sequence of cost function evaluations is converging, it is required that

$$J_k - J_{k-1} < \theta_k \ , \qquad (23)$$

where

$$\theta_k = \tau_F \left(1 + |J_k| \right) , \tag{24}$$

and

$$\| u_k - u_{k-1} \|_\infty < \sqrt{\tau_F^-} \left(1 + \| u_k \| \right) . \tag{25}$$

In addition, to ensure that $\nabla_u H_k \approx 0$, it is required that

$$\| \nabla_u H_k \|_\infty \leq \sqrt[3]{\tau_F^-} \left(1 + \| J_k \| \right) . \tag{26}$$

The parameter τ_F corresponds to the number of digits of accuracy desired in the solution. Finally, in order to prevent conditions 23 and 25 from becoming too stringent, the algorithm is also said to have converged if the alternate condition

$$\| \nabla_u H_k \|_\infty \leq \varepsilon_{abs} , \tag{27}$$

is satisfied, where ε_{abs} is a predefined constant.

4.0 Description of Software Developed

A piece of software initially named Optim1, which implements the polynomial material modeling and trajectory optimization algorithms described above, has been developed by AES to run on UNIX machines that use the X Window System for graphics. Software modules in Optim1 were written in a general form that will expedite modifications when these are necessary due to improvement of the modeling and/or trajectory optimization algorithms.

Optim1 features a graphical user interface that allows the user to easily interact with both the modeling algorithm and the trajectory optimization algorithm. The graphical user interface was written using the Open Software Foundation (OSF) MOTIF™ toolkit (Heller, 1991), which makes the program as easy to use as many existing software applications.

Given compression test data, Optim1 can obtain polynomial models for flow stress, grain size, and percent spheroidization. It is believed at AES that polynomial models for the derivative of the percent spheroidization will have to be computed before the trajectory optimization algorithm can be successfully applied to material polynomial models in general. The modeling algorithm is being modified so that Optim1 can be used to obtain models for derivative of percent spheroidization. These modifications are necessary because a usable model for percent spheroidization needs to include two additional independent variables: the second derivative of the strain and the derivative of the temperature.

The trajectory optimization algorithm has been implemented in Optim1 for the case of a Gamma TiAl model described in Appendix A. The code will be modified to allow for general polynomial models of materials as soon as the test data for the derivative of percent spheroidization becomes available.

7

4.1 Optim1 Graphical User Interface

The graphical user interface for Optim1 contains a main window with a menu bar, a message area, and a status bar. All execution messages and error messages will be written by Optim1 to the message area, with the exception of some status messages that will be written to the text fields in the status bar. Several dialog boxes and plot windows complete the user interface. A screen dump of the main window during execution of the trajectory optimization algorithm is presented in Figure 1.
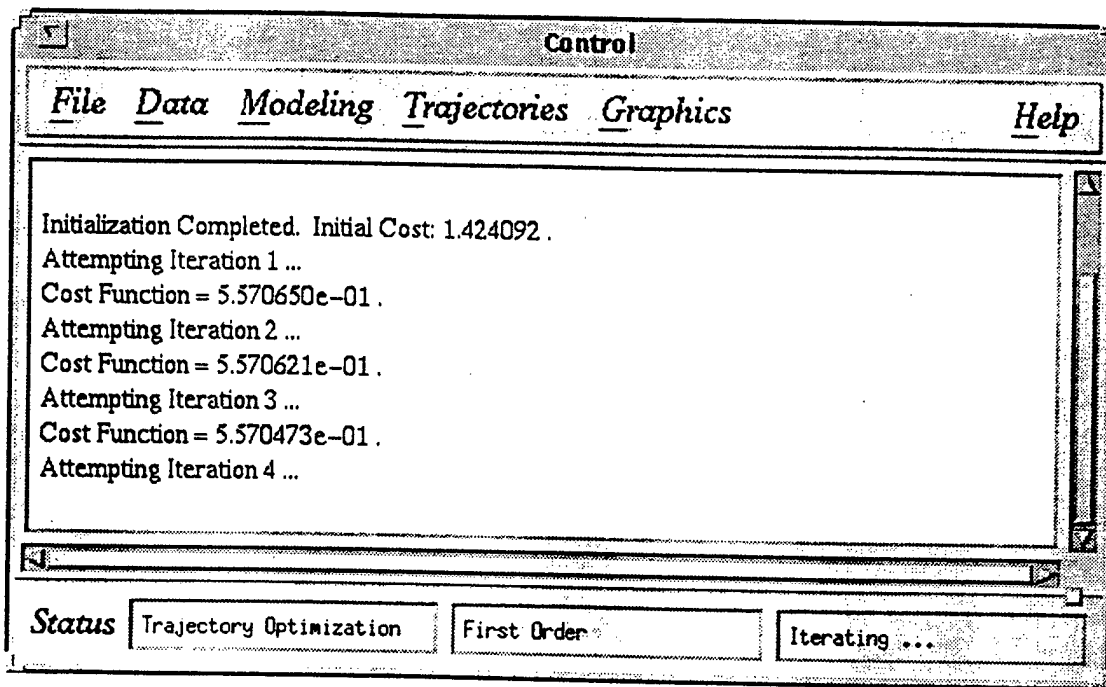

Control

| File | Data | Modeling | Trajectories | Graphics | Help |

Initialization Completed. Initial Cost: 1.424092 .
Attempting Iteration 1 ...
Cost Function = 5.570650e-01 .
Attempting Iteration 2 ...
Cost Function = 5.570621e-01 .
Attempting Iteration 3 ...
Cost Function = 5.570473e-01 .
Attempting Iteration 4 ...

Status | Trajectory Optimization | First Order | Iterating ...

Figure 1. Screen Dump of Optim1 Main Window

4.1.1 Menus and Dialog Boxes

The menu bar at the top of the Optim1 window has several menus: *File, Data, Modeling, Trajectories, Graphics,* and *Help.* Each of these menus has one or more sub menus or options. At the time of writing of this report, help features have not been incorporated to the code.

The *File* menu has six options:

Save Flow Stress Model   A polynomial model for flow stress is saved to a file with extension *.fsm* if such model has been computed. A screen dump of the selection dialog

8
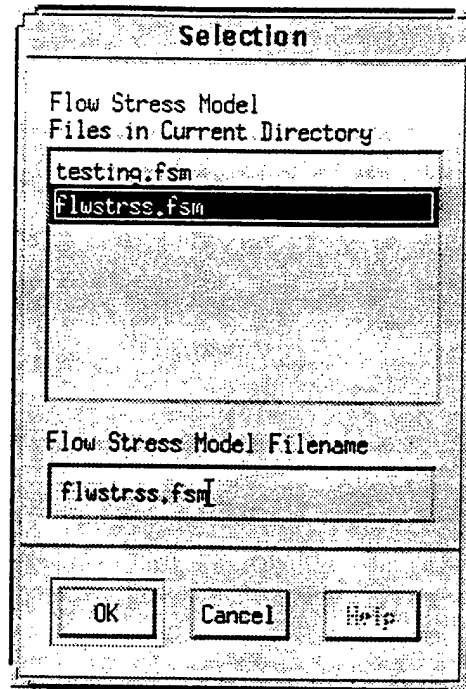
Figure 2. Screen Dump of Dialog Box for Loading/Saving Files

box used for entering the filename is shown in **Figure 2.** Similar dialog boxes are used for all other file load/save procedures.

Save Grain Size Model
A polynomial model for grain size is saved to a file with extension *.gsm* if such model has been computed.

Save Percent Spheroidized Model
A polynomial model for percent spheroidization is saved to a file with extension *.rcm* if such model has been computed.

Save Derivative of Percent Spheroidized Model
A polynomial model for derivative of percent spheroidization is saved to a file with extension *.rdm* if such model has been computed.

Save Trajectory
A strain rate trajectory is saved to a file with extension *.srt* if the trajectory optimization algorithm has been executed.

Quit
Quit Optim1

9

The *Data* menu has four options:

Load Flow Stress Data

> Load compression test data for flow stress. Flow stress data files have extension *.fsd*.

Load Grain Size Data

> Load compression test data for grain size. Grain size data files have extension *.gsd*.

Load Percent Spheroidized Data

> Load compression test data for percent spheroidization. Percent spheroidization data files have extension *.rcd*.

Load Derivative of Percent Spheroidized Data

> Load compression test data for derivative of percent spheroidization. Derivative of percent spheroidization data files have extension *.rdd*.

The *Modeling* menu has four options:

Model Flow Stress

> Generate a polynomial model for flow stress if flow stress data has been loaded.

Model Grain Size

> Generate a polynomial model for grain size if grain size data has been loaded.

Model Percent Spheroidized

> Generate a polynomial model for percent spheroidization if necessary data has been loaded.
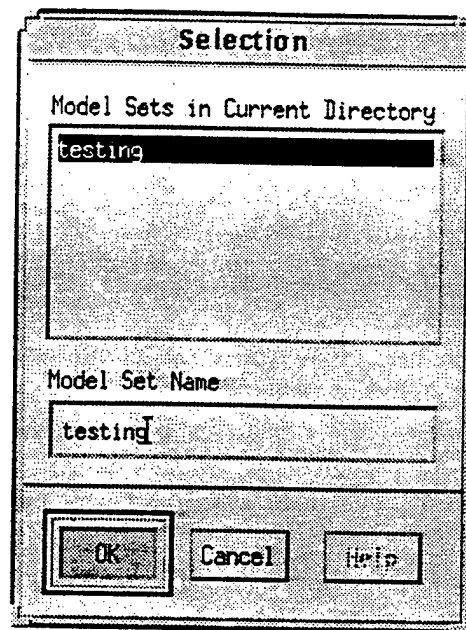
Model Derivative of Percent Spheroidized

> Generate a polynomial model for derivative of percent spheroidization if necessary data has been loaded. This feature is not currently functional, but will be functional as soon as test data for derivative of percent spheroidization becomes available.

The *Trajectories* menu has five options:

Load Model Set

> Load polynomial models for flow stress, grain size, percent spheroidization, and derivative of percent spheroidization. A selection dialog box in which the user can select from the available model sets is drawn to the screen. Figure 3 shows a screen dump of this dialog box.

10

Figure 3. Screen Dump of Dialog Box for Loading Model Sets

Settings

Load/Save/Modify settings for trajectory optimization algorithm. A dialog box that allows the user to input final time, number of time points, initial guess for strain rate, desired values, weights, and some settings for the trajectory optimization algorithm is mapped to the screen. This dialog box is pictured in Figure 4.

First Order, Polynomial Models

First order trajectory optimization algorithm applied to general polynomial models. This option will be functional when models for derivative of percent spheroidization become available. This feature is not currently functional.

First Order, GammaTiAl

First order trajectory optimization algorithm applied to a Gamma TiAl model (see appendix for details of this model). A dialog box in which the user can select to run one or several iterations in the trajectory optimization algorithm. Figure 5 shows a screen dump of this dialog box

11

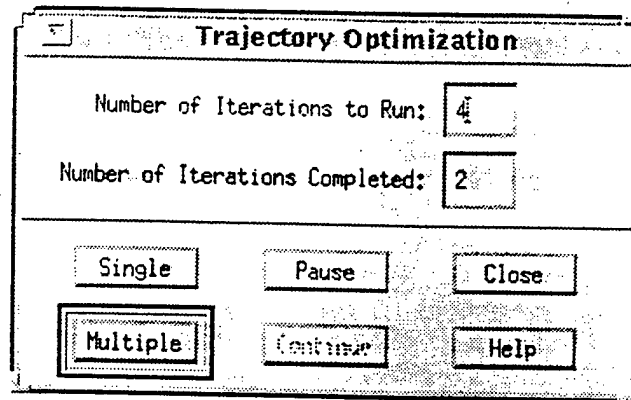**Figure 4. Screen Dump of Trajectory Optimization Settings Dialog Box**

12

Figure 5. Screen Dump of Trajectory Optimization Dialog Box

The *Graphics* menu has two options:

Trajectory Plots   A dialog box for creating two dimensional plots of variables pertinent to the trajectory optimization algorithm is mapped to the screen. The user can create plots of strain, strain rate, grain size, temperature, and percent spheroidization trajectories. Titles and axis labels for trajectory plots are also changeable in this dialog box, which is depicted in Figure 6.

3D Model vs Data Plot

If a model has been obtained for one of the four possible quantities (flow stress, grain size, etc.), a dialog box is created in which the user can choose among several options for various features of a three dimensional plot that compares the data and the obtained polynomial fit. A 3D model vs data plot can be created, updated, and destroyed from this dialog box, which is depicted in Figure 7. At the time of this writing, the plotting package *gnuplot* is used for the model vs data plot. Appendix B gives information about *gnuplot* and its copyright specifics.

The *Help* menu is NOT currently functional.

13

Figure 6. Screen Dump of Dialog Box for Trajectory Plot Definition

Figure 7. Screen Dump of Dialog Box for Model vs Data Plot Control

14

4.1.2 Graphical Output

Several plot windows allow Optim1 to present results to the user, as was already mentioned in the description of the menu system above. These plot windows are created by the user by means of dialog boxes. Variables, titles, and labels for the plots can all be defined before the plots are created.

In the case of the microstructural modeling algorithm, a three-dimensional plot can be created which can be used to verify the agreement between the obtained model and the original test data. A screen dump of the dialog box that controls the three dimensional plots in Optim1 is shown in Figure 7. Figure 8 is a screen dump of a three dimensional plot generated by Optim1 that compares a flow stress model to the corresponding data for a particular temperature.
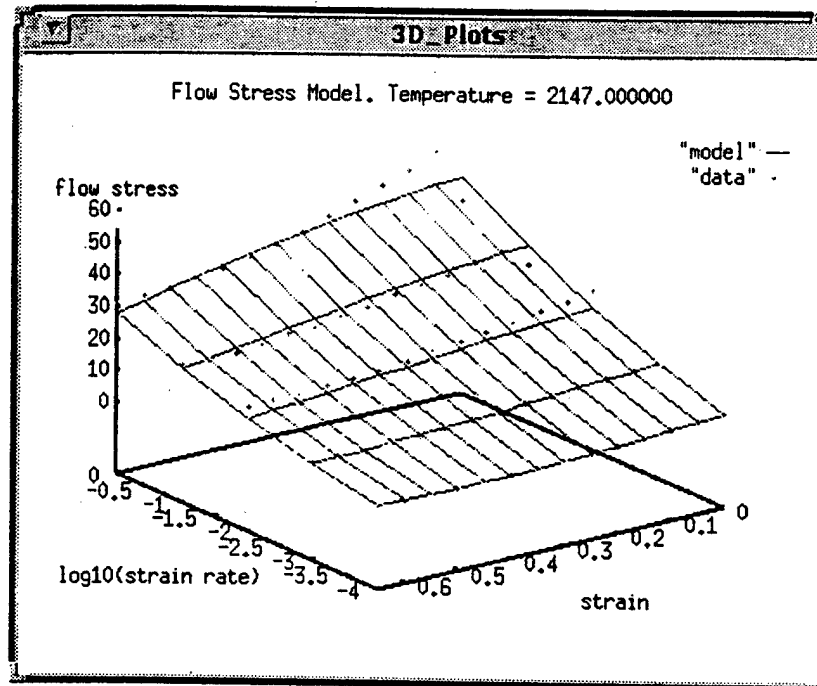

Figure 8.   Screen Dump of a Model vs Data Optim1 3D Plot Window

For the case of the trajectory optimization algorithm, the user can create plots for strain, strain rate, temperature, grain size, and percent spheroidized trajectories, and for the cost function. These plots are updated at each iteration of the algorithm. A screen dump of the dialog box used to create trajectory plots is shown in Figure 6. Figure 9 is a screen dump of a strain rate trajectory plot generated by Optim1 for the model mentioned in Appendix A.
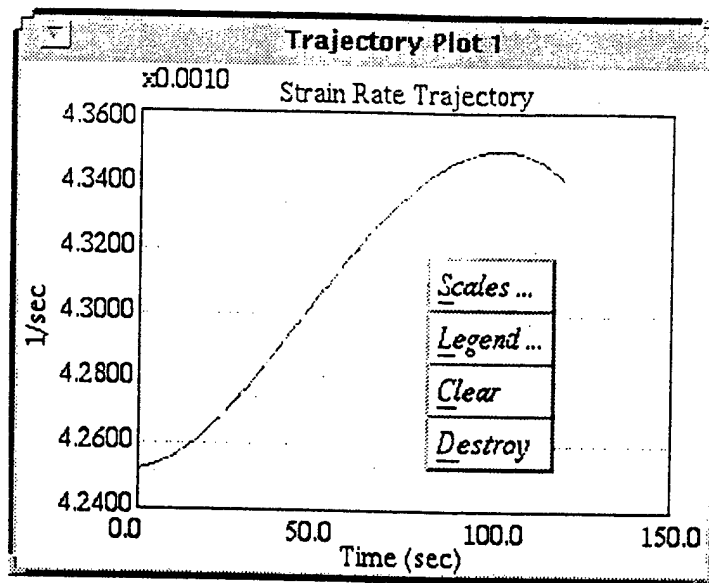
15

Figure 9. Screen Dump of a Strain Trajectory Optim1 Plot Window

5.0 Neutral Data Interface

In the interdisciplinary effort of this SBIR project, it is necessary to exchange data between several algorithms, namely the FE solver, the control algorithm, the trajectory optimization algorithm, and the modeling algorithm. In order to avoid unnecessary modification of all modules when changes to one module are performed, a neutral data interface has been designed so that data transfers take place automatically.

The work reported in this document involved modeling of material behavior and optimization of strain rate trajectories. The data file format issues that affect these two areas of the work are those regarding test data and trajectory data. Files containing polynomial models are expected to be used only as intermediate steps between test data and optimized strain trajectories. However, file formats for all three types of data sets are documented here.

5.1 Optim1 Data File Formats

Optim1 uses data files for four different tasks: input of material test data, input and output of polynomial models, output of designed trajectories, and input and output of settings for the trajectory optimization algorithm. File formats for all these types of files are described in the following sections, with the exception of formats for trajectory

16

optimization settings files, which will never be directly manipulated by the user or by a program other than Optim1.

5.1.1 Material Test Data Files

Two different formats for material test data are used. In the case of flow stress, grain size, and percent spheroidization, the independent variables are strain, strain rate and temperature. The tests are performed at several values of each of these three variables. The following format is used for the files. In this format description, the symbol f represents flow stress, grain size, or percent spheroidization data value, depending on the variable for which data is saved in the file. In the format description, italics represent actual data in the file. Any other letter types and lines that do not begin with italics are comments or pseudo code instructions used here to avoid writing out one line per each piece of data. Each piece of data is written in a separate line in the file.

```
nstrains                integer number of strains in the file
nrates                  integer number of strain rates in the file
ntemps                  integer number of temperatures in the file
for i = 1 to nstrains
  e_i                   ith strain value
end
for i = 1 to nrates
  u_i                   ith strain rate value
end
for i = 1 to ntemps
  T_i                   ith temperature value
end
for i = 1 to ntemps
  for j = 1 to nrates
    for k = 1 to nstrains
      f(e_k, u_j, T_i)  data value for ith temperature, jth strain rate, and kth strain
    end
  end
end
```

In the case of test data for the derivative of percent spheroidization, the independent variables are strain, strain rate, derivative of strain rate, temperature, and derivative of temperature. Since there are five independent variables instead of the three used in the other tests, the data set will be different. The file format used is as follows. All comments given for the case above apply here as well.

```
nstrains                integer number of strains in the file
nrates                  integer number of strain rates in the file
ntemps                  integer number of temperatures in the file
nrders                  integer number of strain rate derivative values in the file
ntders                  integer number of temperature derivative values in the file
for i = 1 to nstrains
```

17

```
    e_i                    ith strain value
  end
  for i = 1 to nrates
    u_i                    ith strain rate value
  end
  for i = 1 to ntemps
    T_i                    ith temperature value
  end
  for i = 1 to ntders
    D_i                    ith temperature derivative value
  end
  for i = 1 to nrders
    R_i                    ith strain rate derivative value
  end
  for i = 1 to nrders
    for j = 1 to ntders
      for k = 1 to ntemps
        for l = 1 to nrates
          for m = 1 to nstrains
            f(e_m, u_l, T_k, D_j, R_i)
```

data value for ith strain rate derivative, jth temperature derivative, kth temperature, lth strain rate, and mth strain

```
          end
        end
      end
    end
  end
```

5.1.2 Files for Polynomial Models

Third degree polynomials in the three variables strain, strain rate, and temperature are used as models for flow stress, grain size, and percent spheroidization. These polynomials have twenty terms. The file format is given below. All conventions given above for other file format descriptions apply here too.

```
nterms                   number of coefficients in the polynomial model (equal to 20 here)
for i = 1 to nterms
  c_i                    ith polynomial coefficient
end
```

For the derivative of percent spheroidization, the model form used is a third degree polynomial in the five independent variables strain, strain rate, temperature, temperature derivative, and strain rate derivative. The format for these files is the same as the format given above for other polynomial models. The number of terms changes to forty six for this case because the number of independent variables is five instead of three.

18

5.1.3 Files for Strain Rate Trajectories

For strain rate trajectories, the variables of interest are the number of points in the trajectory, the time value at each point, and the strain rate value at each point. The format is as follows.

```
npoints                number of points
for i = 1 to npoints
   t_i    u_i          values of time and strain rate for the ith point
end
```

6.0 Selection of Locations for Trajectory Control

The methods that had been proposed for obtaining optimum locations for trajectory control were based on the existence of a hypothetical linear relationship of microstructural quantities from one FEM simulation step to the next. As the derivation of such a relationship would have been computationally prohibitive, these methods were not pursued.

7.0 Conclusions and Recommendations

The tasks assigned to AES under this Phase I SBIR have been successfully performed. Where applicable, file formats have been defined that conform to the neutral data interface philosophy. Algorithms for microstructural modeling and microstructural trajectory optimization have been developed and coded into a menu-driven, graphically oriented program. Methods for choice of locations for ram velocity optimization were studied and found to need excessive computational resources, and therefore these methods were not pursued. Finally, the task of assisting UES in communicating team capabilities to potential consortium members was also performed.

In order for the trajectory optimization algorithm to generate useful results, the models used to characterize the material must be obtained from data that includes dynamic behavior of the material. This type of data is not currently available. It is expected that these results will inspire some efforts for the collection of dynamic data. As soon as these data become available, general polynomial models will be computed and used by Optim1 to generate optimal strain rate trajectories.

Future work includes equipping Optim1 with a cost function editor to help make it unnecessary for the user to become intimately familiar with the mathematical form of the cost function.

Other future work includes the enhancement of microstructure modeling algorithms.

19

43

8.0 References

[1]   Frazier, William G., 1994. Unpublished research and private discussions.

[2]   Heller, D., 1991, Motif Programming Manual for OSF/Motif Version 1.1, First Edition, O'Reilly and Associates, Inc., Sebastopol, California.

[3]   Kirk, Donald E., 1970. Optimal Control Theory, An Introduction, Prentice-Hall Inc., Englewood Cliffs, New Jersey.

[4]   Luenberger, 1984. Linear and Nonlinear Programming, 2nd. ed., Addison Wesley, Reading, Mass.

9.0 Appendices

A.   <u>Gamma TiAl Model in the Current Implementation of the Trajectory Optimization Algorithm</u>

The material model implemented in the current version of Optim1 was obtained with a method similar to that described in Section 2 of this report. Some modifications based on analytical techniques were made to the polynomial models used to test the trajectory optimization algorithm during its development, because the data used to generate the model did not characterize the material dynamics appropriately. It is expected that data that describes material dynamics will be available in the future and general polynomial models will be used to describe material behavior for the trajectory optimization algorithm.

The material model used consists of expressions for the time derivatives of the state variables. Polynomial models of a form slightly different from that described in Section 2 are used to describe the derivatives of percent spheroidized and grain size with respect to time. The derivative of the strain is simply the strain rate. The time derivative of the temperature is described by a simple function of the strain rate and the flow stress. The flow stress is described by a polynomial model of the form given in Section 2. A comparison between a polynomial model for flow stress and the corresponding data is shown in the screen dump of Figure 8.

For the test case, the cost function defined by Equation 5 includes a function h that is the sum of weighted squared differences between actual and desired final values of the state variables. Function g consists of a penalty function based on the hyperbolic tangent function in order to ensure that the strain rate trajectory does not exceed a given maximum value.

Figure 9 is a screen dump of a window that contains a plot of the strain rate trajectory obtained for this example in a test run. The trajectory optimization algorithm converged in four iterations for this case.

B.   <u>Plotting Software Used for the Three-Dimensional Model-vs-Data Plot Option</u>

The three dimensional plots used by Optim1 for comparison of models to test data are implemented by means of a function plotting program called GNUPLOT. The copyright status of Gnuplot is given by the following copyright notice and permission notes. These copyright and permission notes are _applicable only to gnuplot,_ and not to the software written in this SBIR effort.

Copyright (C) 1986-1993 Thomas Williams, Colin Kelley

Permission to use, copy, and distribute this software and its documentation for any purpose with or without fee is hereby granted, provided that the above copyright notice appear in all copies and that both that copyright notice and this permission notice appear in supporting documentation.

Permission to modify the software is granted, but not the right to distribute the modified code. Modifications are to be distributed as patches to released version.

This software is provided "as is" without express or implied warranty.

Copyright and Permission Notices for GNUPLOT

45